




Complex climatic, CO₂, and grazing controls on the net primary productivity and carbon stocks in grasslands of the Tibetan Plateau

Lei Zheng^{a, }, Xiuliang Yuan^b, Guoliang Wang^{a,*, }, Tiancai Zhou^c, Yanyan Pei^d, Shikai Song^e, Yuzhen Li^f, Shihua Zhu^g, Shangyu Shi^a, Jie Peng^h, Yuyang Wangⁱ, Jiaying Zu^j, Xiaoran Huang^b, Qiang Yu^{a,*, }

^a State Key Laboratory of Soil and Water Conservation and Desertification Control, Institute of Soil and Water Conservation, Northwest A&F University, Yangling 712100, China

^b Key Laboratory of Ecological Safety and Sustainable Development in Arid Lands, Xinjiang Institute of Ecology and Geography, Chinese Academy of Sciences, Urumqi 830011, China

^c State Key Laboratory of Tibetan Plateau Earth System, Environment and Resources, Institute of Tibetan Plateau Research, Chinese Academy of Sciences, Beijing 100101, China

^d National Institute of Natural Hazards, Ministry of Emergency Management of China, Beijing 100085, China

^e School of Geographical Sciences, Hebei Normal University, Shijiazhuang 050024, China

^f School of Emergency Management, Xihua University, Chengdu 610039, China

^g Jiangsu Climate Center, Nanjing 210008, China

^h State Key Laboratory of Herbage Improvement and Grassland Agro-ecosystems, College of Ecology, Lanzhou University, Lanzhou 730000, China

ⁱ College of Grassland Science and Technology, China Agricultural University, Beijing 100193, China

^j Key Laboratory of Environment Change and Resources Use in Beibu Gulf, Ministry of Education, Nanning Normal University, Nanning 530001, China

ARTICLE INFO

Keywords:

Carbon dynamics
Biome-BGCMuSo
Climate change
Grassland
Grazing
Tibetan Plateau

ABSTRACT

The Tibetan Plateau (TP) grasslands, the world's largest alpine ecosystem and highest altitude pastoral region, are particularly susceptible to climate change and grazing activities. These alpine grassland ecosystems are experiencing rapid warming, altered precipitation patterns, and changing grazing pressure. However, the relative contributions of climatic factors, CO₂ enrichment, and grazing, and their interactions, to carbon dynamics in these ecosystems remain poorly quantified, which limits our understanding of how these factors affect carbon cycling and feedbacks of alpine ecosystems. Using the process-based biogeochemical model Biome-BGCMuSo integrated with a dynamic grazing module, we conducted multi-scenario simulations to isolate the individual and interactive effects of environmental and anthropogenic factors on carbon dynamics of the TP grasslands over the past 40 years. The results demonstrated that precipitation was the dominant factor in 67.9 % of TP grasslands. Precipitation promoted vegetation growth, increased net primary productivity (NPP) (positive contribution of 54.6 %), enhanced soil carbon inputs (56.6 %), and ultimately drove increases in total carbon (TOTC) (53.1 %). On average, warming alone reduced NPP (negative contribution of -4.6 %) and TOTC (-2.7 %), highlighting its negative impact on carbon stocks. However, when warming occurred with increased precipitation, the combined positive effect on carbon dynamics was found to be more pronounced than that of precipitation alone. This emphasizes the significant interactive effect of temperature and precipitation, where their combined influence enhances carbon sequestration beyond a simple additive response. The effects of CO₂ enrichment, and its interaction with climate change, were both positive and significant, resulting in increased carbon sequestration. Although changes in grazing intensity had a detrimental effect on NPP and TOTC, their impact was comparatively limited. Under the future warming and wetting trend on the TP, alpine grasslands have the potential to sequester more carbon as increasing precipitation, and the interactive effects of warming and wetting, continues to enhance plant growth.

* Corresponding authors.

E-mail addresses: glwang@nwsuaf.edu.cn (G. Wang), yuq@nwfufu.edu.cn (Q. Yu).

<https://doi.org/10.1016/j.catena.2025.109376>

Received 21 April 2025; Received in revised form 13 June 2025; Accepted 11 August 2025

Available online 19 August 2025

0341-8162/© 2025 Elsevier B.V. All rights reserved, including those for text and data mining, AI training, and similar technologies.

1. Introduction

The Tibetan Plateau (TP), with an average altitude of over 4000 m, is characterized by low temperature, low atmospheric pressure and high solar radiation (Ganjurjav et al., 2018). These environmental conditions are critical in shaping the ecological dynamics of the TP. In particular, the TP plays a pivotal role in the global carbon cycle due to its high carbon density and large area, as evidenced by its substantial soil organic carbon (SOC) estimate of 36.6 Pg C (1 Pg = 10^{15} g) (Chen et al., 2020; Ding et al., 2019). Covering an area exceeding 60 % of the TP, the grasslands constitute the most extensive alpine ecosystem in the world (Miehe et al., 2014; Zhou et al., 2024). For millennia, these grasslands have constituted the primary source of pasture for Tibetan communities, thereby establishing the TP as a crucial pastoral region within China (Huang et al., 2017; Zhu et al., 2023a). In addition to their role in sustaining local livelihoods, the grasslands of the TP function as a carbon sink, exhibiting a persistent and potentially enhanced capacity for carbon sequestration (Wang et al., 2023; Wei et al., 2021; Zheng et al., 2023). This underscores the vital function of grasslands of the TP in the mitigation of climate change and in the implementation of carbon management strategies within this ecologically sensitive region.

The carbon cycle processes on the grasslands of the TP are influenced by a number of factors, including atmospheric CO₂ enrichment, changes in the climate, and human activities (Dong et al., 2020; Wang et al., 2022; Zhu et al., 2016). The concentration of CO₂ in the global atmosphere has been rising continuously, reaching 419.3 parts per million (ppm) by 2023 (Friedlingstein et al., 2023). Elevated CO₂ concentrations can stimulate photosynthesis in plants, leading to enhanced growth rates and biomass production, a phenomenon known as the CO₂ fertilization effect (Wang et al., 2020). Over the last several decades, there has been a significant climatic shift in the TP, characterized by warming and increased precipitation (Duan and Xiao, 2015; Wang et al., 2018). The mean annual air temperature of the TP has been observed to exhibit a significant increase over the period between 1980 and 2018. A synthesis of data from multiple sources, including observations and ten gridded air temperature products, indicates that the rate of this increase is 0.45 ± 0.09 °C decade⁻¹ (based on observations), and 0.24 ± 0.10 °C decade⁻¹ to 0.48 ± 0.10 °C decade⁻¹ (based on different gridded products) (Peng et al., 2021b). From 1961 to 2012, precipitation exhibited a general increase at a rate of 5.07 mm decade⁻¹, with a trend that varied across seasons and exhibited notable spatial heterogeneity (Wang et al., 2018). In addition to atmospheric CO₂ enrichment and climatic changes, anthropogenic influences have also impacted the alpine grasslands. There was a 16.1 % reduction in human activity intensity on the TP between 2000 and 2017, which can be attributed to the implementation of recent ecological conservation policies (Li et al., 2021c). Grazing is the dominant human activity on the TP. This makes it a key indicator for assessing the overall intensity of anthropogenic impacts on grassland ecosystems (Huang et al., 2016). The dynamics of carbon in grasslands are influenced by a combination of these natural and anthropogenic factors. These influences are characterized by complex interactions that cannot be accurately represented by simple additive effects (Fang et al., 2019). Consequently, a major challenge remains in determining the relative contributions of these drivers and understanding their spatial heterogeneity across the TP (Zhu et al., 2023b). The dominant driver of grassland carbon dynamics on the TP remains unclear. For instance, Shi et al. (2023) suggested that temperature and precipitation are the primary controlling factors, while Zhao et al. (2022) suggested that grazing plays a more significant role. The absence of a quantitative analysis of multi-factor interactions has hindered a mechanistic understanding of regional carbon sink dynamics. The controversy stems from the lack of quantification of multi-factor interactions, particularly the interactive of climatic factors (temperature and precipitation) and CO₂ fertilization, which has not been clearly disentangled. In order to develop effective carbon sequestration management policies for TP grasslands under the influence of multiple environmental drivers, it is crucial to develop

modelling approaches to isolate and quantify the individual and interactive effects of climate change, CO₂ fertilization, and grazing activities on carbon dynamics.

Frequently employed methodologies to evaluate the effects of climate change and human activities on alpine grasslands at the regional scale are traditional statistical analyses and the Residuals-Trend model (Li et al., 2018a). Traditional statistical analyses employ remote sensing data, climate data, and socio-economic statistics for the quantitative assessment of the impact of climate change and human activities on grassland ecosystems. The interrelationships between climate factors, human activities and vegetation indices are investigated through the application of analytical techniques such as correlation analysis, partial correlation analysis and, generalized linear models (Li et al., 2018b; Xiong et al., 2021; Yu et al., 2021). However, the spatially heterogeneous impacts of human activities on alpine grasslands cannot be fully captured by spatial socio-economic statistics (Li et al., 2018a). Moreover, the majority of analogous statistical analyses have not incorporated CO₂ fertilization as an independent variable in their assessments. Another commonly employed approach is the Residuals-Trend models, used in studies of climatic and anthropogenic factors on alpine grasslands, particularly on the TP (Huang et al., 2016; Pan et al., 2017; Wang et al., 2016; Zhou et al., 2024). The Residuals-Trend model typically comprise two models: one for calculating potential vegetation growth and the other for calculating actual vegetation growth. Actual vegetation growth can be simulated using e.g. the Carnegie-Ames-Stanford Approach (CASA) model with remote sensing data (Zhou et al., 2024). Potential vegetation growth can be simulated by process-based models (Chen et al., 2014). The impact of human activities can be inferred by contrasting actual and potential vegetation growth. The Residuals-Trend model assumes that potential vegetation growth is exclusively driven by climate change. The Residuals-Trend model has inherent limitations, including discrepancies between the two models. These discrepancies contribute to the uncertainty of the results of the assessment. Moreover, the Residuals-Trend model is only applicable to retrospective analyses of vegetation dynamics. Thus, it is unable to assess the impacts of climate change and anthropogenic activities on carbon sequestration potential or to predict future ecological changes. Thus, current approaches are constrained by two main limitations: (1) an inadequate representation of CO₂ fertilization and grazing impacts (either due to the omission of grazing modules or using coarse-resolution socioeconomic data), and (2) a focus on vegetation dynamics which fails to account for the underlying mechanisms of carbon sequestration.

In contrast to the aforementioned methods, process-based ecosystem models, validated against field observations, provide a more reliable approach for evaluating the impacts of CO₂ fertilization, climate change, and human activities on alpine grasslands. Using multi-scenario simulations enables to isolate the effects of individual factors and their interactions, as well as to elucidate the spatial-temporal patterns of carbon dynamics in response to these factors (Chang et al., 2016; Zhu et al., 2023b). These models facilitate a comprehensive analysis of various environmental and anthropogenic factors at the regional scale, offering valuable insights into their complex interactions with ecosystem dynamics (Sitch et al., 2024). Such analyses are particularly relevant for the grasslands of the TP, where grazing is a dominant anthropogenic influence (Huang et al., 2016). They can inform the selecting grazing-related indicators and the determination of their weights within ecological assessment frameworks. However, since many current ecosystem process-based models do not include a grazing module, grazing effects on alpine grassland ecosystems cannot be conceptualized, parameterized, and quantified (Zhu et al., 2022). In this study, we employed a process-based biogeochemical model, Biome-BGCMuSo, which has been specifically enhanced with an improved phenological model for the TP (Zheng, 2022; Zheng et al., 2022). Further, we combined the Biome-BGCMuSo model, integrated with a dynamic grazing module, with our 0.1° spatial data on grazing intensity, enabling us to quantitatively assess grazing impacts on carbon dynamics

of alpine grasslands on the TP (Hidy et al., 2012). Then, the Biome-BGCMuSo model was used to assess the relative contributions of different environmental factors to the carbon dynamics of grasslands on the TP by designing a series of simulation scenarios, overcoming the limitations of traditional single-factor analysis approaches to isolate multifactorial interactions. Therefore, the objective of this study was (1) to quantify the individual and interactive contributions of climatic drivers (i.e. precipitation and temperature changes), CO₂ fertilization, and grazing activities to carbon dynamics in the grasslands of the TP; and (2) to generate regional-scale maps illustrating the spatial heterogeneity of these dominant environmental drivers, providing insights into their varying influence across the TP grasslands.

2. Methods and datasets description

2.1. Study area

The Tibetan Plateau (TP), also referred to as the Qinghai-Tibetan Plateau, has an average altitude exceeding 4000 m, making it the highest plateau on Earth. Most of the annual precipitation occurs during the summer months, and there is a gradient of annual precipitation sums towards the southeast, from a minimum of less than 100 mm to a maximum of more than 700 mm (Yang et al., 2010). 54 % of the region has an annual precipitation below 400 mm (Peng et al., 2021a). The mean annual temperature on the TP ranged from −15 °C to 5 °C, with 67 % of the area experiencing annual temperatures below 0 °C (Peng et al., 2021a; You et al., 2013). Different types of grasslands can be found based on the precipitation gradient, including alpine meadows in the east (characterized by a semi-decomposed residual turf with tightly interwoven root mats) and alpine steppes in the west and middle (characterized by grasses and shrubs that are extremely cold and drought-tolerant) (Feng and Squires, 2020) (Fig. 1). The TP is home to a significant number of livestock, which rely on the region's grasslands as a source of sustenance. The number of large livestock, sheep, and goats in Qinghai Province (hereafter referred to as Qinghai) and Tibetan Autonomous Region (hereafter referred to as Tibet) reached 12.02 million, 19.07 million, and 5.67 million in 2017, respectively (Li et al., 2021a).

2.2. Model description

This study employed Biome-BGCMuSo (version 6.1), an enhanced version of the Biome-BGC model, to simulate the storage and exchange of water, carbon, and nitrogen among the vegetation, litter, and soil

components of terrestrial ecosystems (Hidy et al., 2016). The Biome-BGCMuSo model simulates ecological processes on a daily time step, driven by key meteorological inputs including daily maximum and minimum temperatures, precipitation, solar radiation, and VPD. In comparison to Biome-BGC, Biome-BGCMuSo incorporates a number of structural enhancements, including the replacement of the single-layer soil module with a multilayer soil module and the incorporation of a soil moisture-dependent senescence module. Furthermore, the model provides a variety of management modules for cropland, forest, and grassland ecosystems, enabling more precise simulations of human activities (Hidy et al., 2022). The grazing module quantifies plant material consumption based on the key parameter of stocking rate. It also accounts for biomass redistribution through excretal returns to the litter pool. The detailed methodology for calculating grazing effects and biomass fluxes was presented in Hidy et al. (2012). Since the grasslands on the TP are located in alpine conditions, capturing their seasonal dynamics is challenging (Sun et al., 2017a). In order to enhance the simulation of vegetation seasonal growth dynamics, new phenological models were incorporated into Biome-BGCMuSo. Additionally, parameters were optimized using a particle swarm optimization (PSO) algorithm, calibrated against remotely-sensed dates for the start and end of the growing season (Zheng et al., 2022). The spin-up simulations of the Biome-BGCMuSo were run for a maximum of 3200 years, and the transient simulations for 240 years in this study. For the analysis of interannual variability, net primary productivity (NPP, g C m^{−2} a^{−1}) was output as an annual value. SOC (g C m^{−2}), vegetation carbon (VEGC, g C m^{−2}) and litter carbon (LTRC, g C m^{−2}) were derived from daily output values and averaged over the year. The aboveground biomass (AGB, g C m^{−2}) was extracted on 15 August, representing the peak of the growing season. All these variables were produced at a spatial resolution of 0.1°.

2.3. Model input data

To drive the Biome-BGCMuSo model, we used several datasets including meteorological, soil, topographic and grazing data. (a) Meteorological data: Daily regional meteorological variables, including precipitation, shortwave radiation, and daily minimum, maximum, and mean temperatures were obtained from the China Meteorological Forcing Dataset (CMFD) (He et al., 2020), covering the period from 1979 to 2018 at a spatial resolution of 0.1°. The daily photoperiod and vapor pressure deficit (VPD) were calculated using the MTCLIM model (Bohn et al., 2013). (b) Soil texture data, including the percentages of sand, silt, and clay, and pH values, were derived from the China Soil Characteristics Dataset (2010) (Shangguan et al., 2012). (c) Elevation data were obtained from the Shuttle Radar Topography Mission (SRTM) v4.1 Digital Elevation Model (DEM). (d) Pasture distribution and grazing intensity data: We used the altitude division criteria proposed by Wang et al. (2010) for seasonal pastures in eight prefecture-level divisions in Qinghai Province (hereafter referred to as Qinghai). In the six prefecture-level divisions in the Tibetan Autonomous Region (hereafter referred to as Tibet), we dynamically adjusted the altitude criteria for pasture division in the cold and warm seasons to ensure that the final distribution of seasonal pastures is consistent with the pasture area ratio in the cold and warm seasons as determined by the comprehensive scientific expedition team of the Qinghai Tibet Plateau, Chinese Academy of Sciences (1992). Distribution of pastures in the cold and warm seasons in Xinjiang Autonomous Region (hereafter referred to as Xinjiang) was obtained from Zhu et al. (2022). Since there are no altitude division criteria for Sichuan (hereafter referred to as Sichuan), Yunnan Province (hereafter referred to as Yunnan), and Gansu province (hereafter referred to as Gansu), the nearby regions of Tibet and Qinghai were used as a reference for determining pasture distribution in the cold and warm seasons. The distribution of summer pasture and winter pasture on the TP was mapped using area ratios of different pasture types in alpine meadows or alpine steppes within the 0.1° grid (Fig. S1). The Gridded Livestock of the World (GLW3) database (Gilbert et al.,

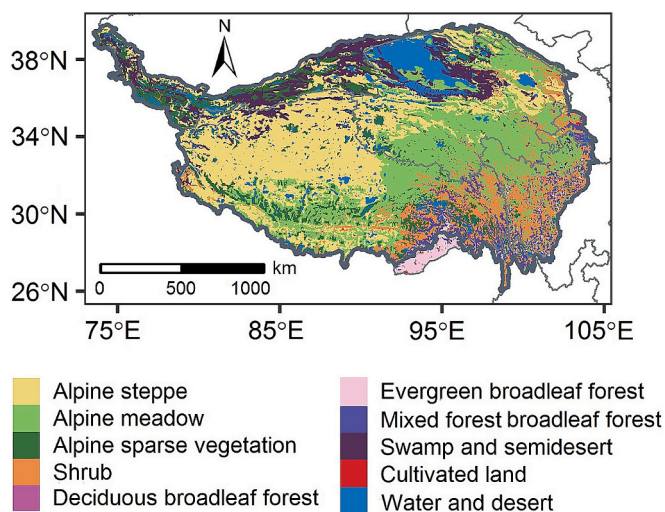


Fig. 1. The land cover types on the Tibetan Plateau (TP), extracted from the Vegetation Maps of China at a scale of 1:1000000.

2018) was interpolated and adjusted using livestock numbers from a variety of regional statistical yearbooks, along with sequence data of livestock number at county level on the Tibetan Plateau and the data on livestock products from the Tibetan Autonomous Region, obtained from the National Tibetan Plateau Data Center (<https://data.tpdc.ac.cn/>). The **Supplementary Text S1** and **Figs. S2, S3, S4** presents more detailed information about the process of generating grazing intensity data.

2.4. Model evaluation

The performance of Biome-BGCMuSo was evaluated by comparing model output to observed and derived data, using a combination of AGB, NPP, and SOC. The field-observed AGB was measured at 115 sites across the TP during the peak vegetation growth period from late July to mid-August 2015. The plant samples were sun-dried in the field and subsequently oven-dried in the laboratory at 65 °C until a constant weight was achieved. The dry matter AGB was converted to units of g C m⁻² using a conversion factor of 0.45 (Sun et al., 2017b). The spatial distribution of the sampling sites, which span different aridity gradients across the TP and are highly representative of the region, can be found in Sun et al. (2019). Specifically, 66 sampling sites are located in alpine steppe, and 49 sampling sites are located in alpine meadow (Fig. S5). Regional-scale AGB data from Zeng et al. (2019) were used to validate the Biome-BGCMuSo model at the regional level. These data were monitored by a random forest (RF) algorithm, incorporating 256 field-observed AGB, topographical data, meteorological data (temperature and precipitation), and remote sensing vegetation indices. The spatial AGB data at a resolution of 1 km × 1 km were aggregated to 0.1° × 0.1° resolution by averaging for model use. Annual NPP estimates were obtained from the MODIS NPP dataset (MOD17A3H) at a spatial resolution of 500 m (Running and Zhao, 2015), enabling consistent evaluation of ecosystem productivity across the TP. SOC was obtained from the National Tibetan Plateau Data Center (<https://data.tpdc.ac.cn/>) as a gridded dataset. It was generated by using a RF algorithm to generate gridded maps of carbon stocks across the region at a spatial resolution of 5 km (Han et al., 2022). The input to the RF algorithm was 7196 sample plots, collected from the 1980 s to 2020 and encompassing a diverse range of soil types and ecological conditions. The NPP and SOC datasets were aggregated to a 0.1° × 0.1° resolution by averaging, thus enabling comparison with the model outputs. To further assess the spatial patterns of the model simulations, we incorporated the aridity zones, which are defined based on the aridity index (AI): arid (AI < 0.20), semi-arid (0.20 ≤ AI < 0.50), dry sub-humid (0.50 ≤ AI < 0.65), and humid (AI ≥ 0.65), enabling the differentiation of results across varying aridity levels (Fig. S6). The Aridity Index was sourced from the Global Aridity Index and Potential Evapotranspiration (ET0) Climate Database v2 (Trabucco and Zomer, 2019).

In order to evaluate the performance of the model simulations, two commonly used evaluation measures are employed: the coefficient of determination (R²) and the root mean square error (RMSE). These are defined below:

$$R^2 = \frac{\sum_{i=1}^n (S_i - \bar{O})^2}{\sum_{i=1}^n (O_i - \bar{O})^2} \quad (1)$$

$$RMSE = \sqrt{\frac{\sum_{i=1}^n (O_i - S_i)^2}{n}} \quad (2)$$

where S_i and O_i represent the i th simulated values of AGB from the Biome-BGCMuSo simulations and the corresponding field-observed values, respectively. For regional-scale evaluation, S_i represents the i th simulated NPP or SOC value from the Biome-BGCMuSo simulations, while O_i represents the corresponding MODIS NPP or SOC value monitored by a RF algorithm, serving as the observed data. \bar{O} is the mean of observed values, and n denotes the total number of observations.

2.5. Factorial experiments and contributions of each driver to carbon dynamics

In order to assess the relative contributions of various environmental factors to AGB, NPP, SOC, VEGC, LTRC, and total carbon (TOTC, defined as the sum of SOC, VEGC, and LTRC), a series of simulation experiments under different scenarios were conducted (Table 1). Furthermore, factor analysis was employed to disentangle both the individual and interactive effects of multiple environmental drivers (Zhu et al., 2023b). The eight distinct scenarios designed for this analysis were as follows: (1) $S_{OVERALL}$ simulates carbon dynamics under actual environmental conditions, including climate change, atmospheric CO₂ enrichment, and changes in grazing intensity. (2) $S_{CO2fert}$ represents a scenario where the concentration of CO₂ is the sole variable, while all other climate factors and grazing intensity are held constant. (3) S_{CLIM} simulates climate change while maintaining CO₂ levels and grazing intensity at their 1979 baseline. (4) $S_{CO2CLIM}$ represents a scenario in which only the grazing intensity remains constant and other climate factors and CO₂ levels change. (5) S_{PREC} represents a scenario where precipitation is the sole variable, while temperature, grazing intensity, and CO₂ levels are held constant. (6) S_{TEMP} represents a scenario where only temperature changes (including mean, maximum, and minimum values), while precipitation, grazing intensity, and CO₂ levels are held constant. (7) $S_{GRAZING}$ represents a scenario where only the grazing intensity changes, while other climate factors and CO₂ are held constant. (8) $S_{CONTROL}$ represents a scenario where the grazing intensity, climate factors, and CO₂ levels are held constant. The changes in AGB, NPP, and SOC were determined by comparing the mean simulated values corresponding to the periods 1999–2018 and 1979–1988. The specific formulae are as follows:

$$OVERALL_{effect} = VAR_{1999-2018, OVERALL} - VAR_{1979-1998, OVERALL} - CTRL_{effect} \quad (3)$$

$$TEMP_{effect} = VAR_{1999-2018, TEMP} - VAR_{1979-1998, TEMP} - CTRL_{effect} \quad (4)$$

$$PREC_{effect} = VAR_{1999-2018, PREC} - VAR_{1979-1998, PREC} - CTRL_{effect} \quad (5)$$

$$CO2fert_{effect} = VAR_{1999-2018, CO2fert} - VAR_{1979-1998, CO2fert} - CTRL_{effect} \quad (6)$$

$$CLIM_{effect} = VAR_{1999-2018, CLIM} - VAR_{1979-1998, CLIM} - CTRL_{effect} \quad (7)$$

$$CO2CLIM_{effect} = VAR_{1999-2018, CO2CLIM} - VAR_{1979-1998, CO2CLIM} - CTRL_{effect} \quad (8)$$

$$GRAZING_{effect} = VAR_{1999-2018, GRAZING} - VAR_{1979-1998, GRAZING} - CTRL_{effect} \quad (9)$$

$$CO2 \leftrightarrow CLIM_{effect} = CO2CLIM_{effect} - CLIM_{effect} - CO2fert_{effect} \quad (10)$$

$$PREC \leftrightarrow TEMP_{effect} = CLIM_{effect} - TEMP_{effect} - PREC_{effect} \quad (11)$$

$$CTRL_{effect} = VAR_{1999-2018, CONTROL} - VAR_{1979-1998, CONTROL} \quad (12)$$

where VAR refers to simulated AGB, NPP, and carbon stocks; the interactive effects between climate and CO₂ change are denoted by $CO2 \leftrightarrow CLIM_{effect}$; the interactive effect between precipitation and temperature are denoted by $PREC \leftrightarrow TEMP_{effect}$. The first part of the VAR suffix signifies the temporal duration (e.g., 1979–1998), whereas the latter part specifies the specific experimental scenario (Table 1).

The relative contribution (RC) of each driver to the total change in AGB, NPP, and carbon stocks can be determined with the following equation:

$$RC_i = \frac{Effect_i}{\sum_{j=1}^6 |Effect_j|} \times 100\% \quad (13)$$

Table 1
Experimental design.

Scenarios	Climate factors		Grazing intensity	CO ₂	Experimental description
	Precipitation	Temperature ^a			
S _{OVERALL}	Transient ^b	Transient	Transient	Transient	Combined effect
S _{CO2fert}	Equilibrium ^c	Equilibrium	1979	Transient	Single factor effect (CO ₂)
S _{CLIM}	Transient	Transient	1979	1979	Climate change effect
S _{CO2CLIM}	Transient	Transient	1979	Transient	CO ₂ and climate change effect
S _{PREC}	Transient	Equilibrium	1979	1979	Single factor effect (Precipitation)
S _{TEMP}	Equilibrium	Transient	1979	1979	Single factor effect (Temperature)
S _{GRAZING}	Equilibrium	Equilibrium	Transient	1979	Single factor effect (Grazing intensity)
S _{CONTROL} ^d	Equilibrium	Equilibrium	1979	1979	Control experiment

^a Temperature indicates the maximum, minimum, and mean temperature.

^b Transient represents that model is driven by historical data during 1979 to 2018.

^c Equilibrium is constituted by the mean climate state from 1979 to 1988. Equilibrium temperature data was generated using the average temperature data from 1979 to 1988. We calculated equilibrium precipitation data by multiplying the annual precipitation for each year between 1979 and 2018 by the adjustment factor so that the annual precipitation for each year is equal to the average annual precipitation between 1979 and 1988.

^d The control experiment was carried out. CTRL_{effect} represents the inherent variability of the ecosystem process-based model when driven by equilibrium meteorological data. This allows us to account for and subtract the baseline variability of the model, thereby isolating the true effects of external forcing on AGB, NPP, and carbon stocks.

where Effect_{*i*} denotes the individual contribution of driver *i* (the PRE_{effect}, TEMP_{effect}, CO₂fert_{effect}, GRAZING_{effect}, PREC ↔ TEMP_{effect}, and CO₂ ↔ CLIM_{effect}). The sign of RC_{*i*} indicates the direction of its contribution to changes in AGB, NPP, and carbon stocks: a positive value indicates an increase in these variables, while a negative value indicates a decrease in these variables.

3. Results

3.1. Performance evaluation of Biome-BGCMuSo

The Biome-BGCMuSo model was validated against the previously described datasets of AGB, NPP and SOC (see Section 2.4 for details). The comparison to field-observed AGB demonstrated moderate agreement, with an R² of 0.53 and a root mean square error (RMSE) of 38.37 g C m⁻² (Fig. 2). The Biome-BGCMuSo model demonstrated a better

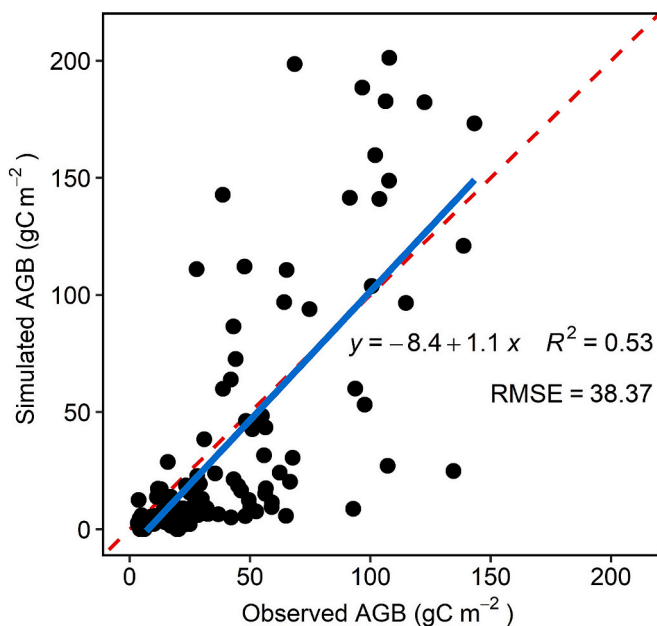


Fig. 2. Scatterplot comparing observed aboveground biomass (AGB) with simulated AGB in 2015.

performance in capturing regional AGB variability, achieving a higher R² of 0.65 and a reduced RMSE of 29.42 g C m⁻² when compared with the AGB estimated using a RF algorithm (Fig. 3c4). The regional average AGB estimated by the RF algorithm and simulated by the Biome-BGCMuSo were 36.21 g C m⁻² and 37.22 g C m⁻², respectively. In the case of SOC, the comparison exhibited an R² of 0.56 and an RMSE of 11.02 kg C m⁻² (Fig. 3a4). However, the simulated mean SOC (12.08 kg C m⁻²) across the grasslands of the TP was found to be lower than the mean estimated by the RF algorithm (14.49 kg C m⁻²). Finally, with respect to MODIS NPP, the model exhibited an R² of 0.60 and an RMSE of 86.32 g C m⁻², with the estimated regional mean (120.49 g C m⁻²) being slightly lower than the MODIS-derived mean (129.68 g C m⁻²) (Fig. 3b4). The model reproduced the general variability of NPP at the regional scale. It effectively captured the observed declining trends of SOC, NPP, and AGB from southeast to northwest across the grasslands of the TP (Fig. 3a1, a2, b1, b2, c1, c2). Furthermore, the model successfully reproduced variations in SOC, NPP, and AGB along aridity gradients (Fig. 3a3, b3, c3, and Fig. S6). The simulated NPP exhibited an increase from arid to humid zones, peaking in the humid zones, which closely aligned with the MODIS NPP trends (Fig. b3). For SOC and AGB, the model demonstrated an overall increasing trend in accordance with the aridity index, although there were also systematic deviations compared to the RF-estimated SOC and AGB. Specifically, there were underestimations in arid zones (low aridity index) and overestimations in humid zones (high aridity index) relative to the RF-estimated SOC and AGB, indicating the potential for bias in the SOC and AGB simulations of the Biome-BGCMuSo (Fig. 3a3, c3).

3.2. Effects of different factors on AGB, NPP and carbon stocks

Under the S_{OVERALL}, notable temporal variation in carbon dynamics was observed in the TP grasslands over the past 40 years. TOTC, total soil organic carbon (TOTSOC), total carbon above 30 cm soil depth (TOTC30), top layer (0–30 cm) soil organic carbon (SOC30), LTRC, and VEGC all showed significant increases, with rate of 6.5 g C m⁻² a⁻¹, 4.5 g C m⁻² a⁻¹, 5.2 g C m⁻² a⁻¹, 3.2 g C m⁻² a⁻¹, 0.8 g C m⁻² a⁻¹, and 0.5 g C m⁻² a⁻¹, respectively (Fig. 4). AGB and NPP increased significantly by 0.2 g C m⁻² a⁻¹ and 1.3 g C m⁻² a⁻¹ respectively, with minimum values of 23.5 g C m⁻² and 77.3 g C m⁻² a⁻¹ in 1995. The mean values of each carbon pool, NPP, and AGB for the period 2000–2018 under different scenarios were compared to the S_{CONTROL} scenario for the same time period in order to assess the effects of individual and interactive influences of climatic factors, atmospheric CO₂ enrichment, and grazing

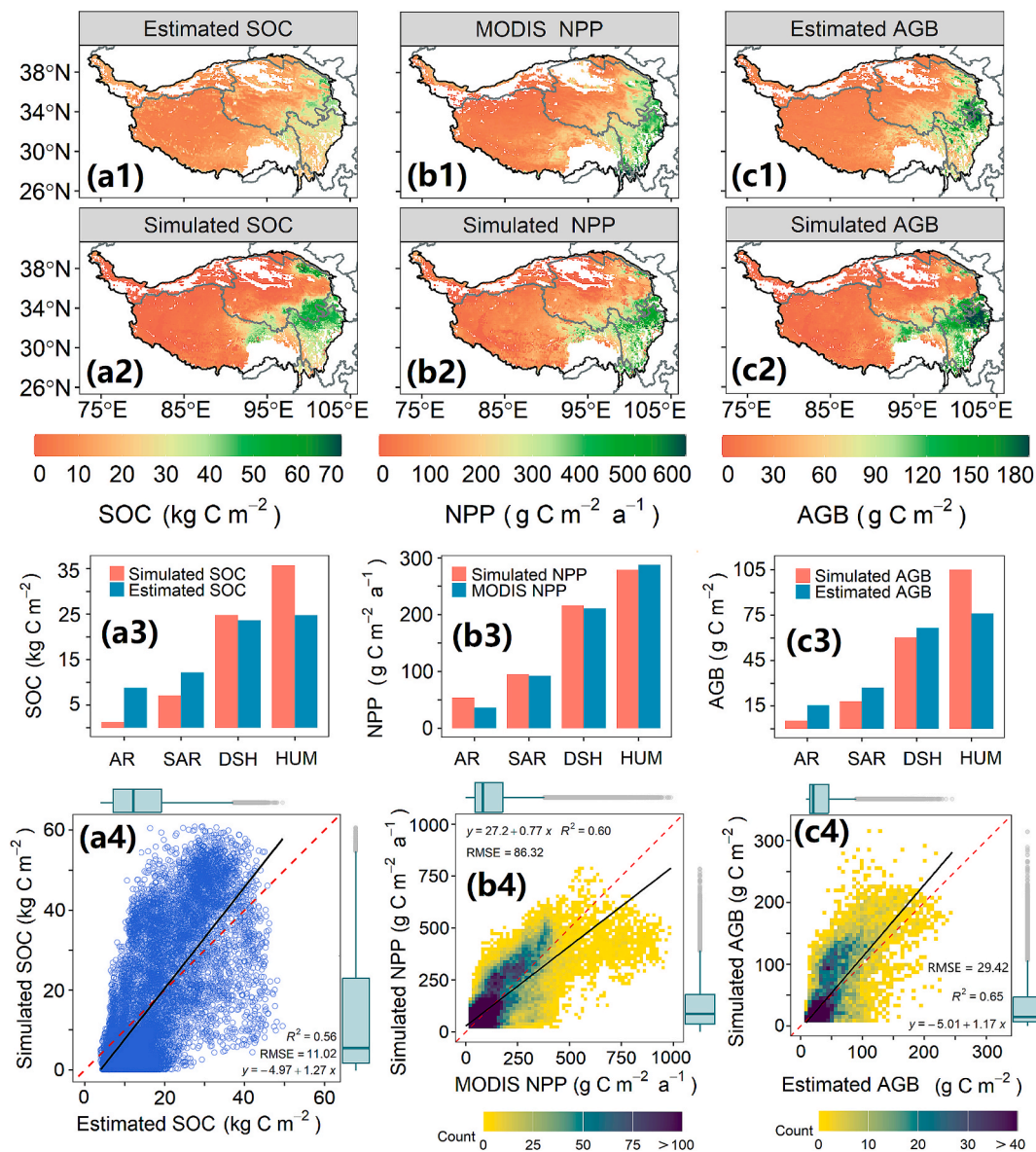


Fig. 3. Spatial distribution maps: estimated soil organic carbon (SOC) using a random forest (RF) algorithm (a1), simulated SOC (a2), MODIS net primary productivity (NPP) (b1), simulated NPP (b2), estimated AGB using a RF algorithm (c1), and simulated AGB (c2). Changes in regional averages based on aridity zones: SOC (simulated in Coral Red and RF-estimated in Cyan Blue) (a3), NPP (simulated in Coral Red and MODIS in Cyan Blue) (b3), and AGB (simulated in Coral Red and RF-estimated in Cyan Blue) (c3). The aridity zones are defined based on the aridity index (AI): AR (Arid, $AI < 0.20$), SAR (Semi-arid, $0.20 \leq AI < 0.50$), DSH (Dry Sub-humid, $0.50 \leq AI < 0.65$), and HUM (Humid, $AI \geq 0.65$). Scatterplot comparing estimated SOC with simulated SOC, averaged over 1978–2018 (a4). Scatterplot comparing MODIS NPP with simulated NPP (b4). The comparison was conducted over three time periods: 2001–2005, 2006–2010, and 2011–2015, with the MODIS NPP and simulated NPP averaged for each period. Each point in the scatter plot represents a spatial grid cell, where the averaged MODIS NPP is compared to the corresponding simulated NPP for the same period. All three time periods are displayed together in the scatterplot to evaluate temporal consistency between the MODIS estimates and model simulations. Scatterplot comparing estimated AGB with simulated AGB, averaged over 2000–2014 (c4).

(Fig. 4 and Table 2). Under the CO₂ fertilization scenario (S_{CO₂fert}), all carbon pools, NPP, and AGB increased, with TOTC (defined as the sum of SOC, LTRC, and VEGC) rising by 32.4 g C m⁻², NPP by 6.4 g C m⁻² a⁻¹, and AGB by 2.6 g C m⁻². However, the effect of CO₂ fertilization (CO₂fert_{effect}) was less pronounced than that of precipitation changes alone. In comparison to S_{CONTROL}, S_{PREC} resulted in notable increases in each carbon pool, NPP, and AGB, with TOTC rising by 89.2 g C m⁻², NPP by 21.6 g C m⁻² a⁻¹, and AGB by 5.3 g C m⁻². Precipitation was identified as the primary factor driving the increase in carbon stocks, NPP, and AGB. When compared with S_{CO₂fert}, S_{TEMP}, and S_{GRAZING} scenarios, the individual effect of precipitation (PREC_{effect}) was the most pronounced among all scenarios. The S_{TEMP} scenario demonstrated slight increases in TOTC, TOTC30, TOTSOC, SOC30, and NPP in comparison to

S_{CONTROL}. Conversely, VEGC, LTRC, and AGB exhibited slight decreases. While the impact of temperature on vegetation was negative, with reductions in VEGC, LTRC, and AGB, the combined effects of precipitation and temperature changes were positive. Under the S_{CLIM} scenario, there were notable increases in VEGC, LTRC, and AGB, which were more pronounced than those simulated in the S_{PREC} scenario. In particular, VEGC increased by 23.2 g C m⁻², LTRC by 7.6 g C m⁻², and AGB by 5.9 g C m⁻². These findings suggest that the interactive effects of precipitation and temperature (PREC ↔ TEMP_{effect}) play a significant role in promoting plant growth. In the S_{CO₂CLIM} scenario, increases in carbon pools, NPP, and AGB were greater than the sum of the increases in the S_{CO₂fert} and S_{CLIM} scenarios. This suggests that the interactive effects between climate factors and CO₂ (CO₂ ↔ CLIM_{effect}) enhance carbon

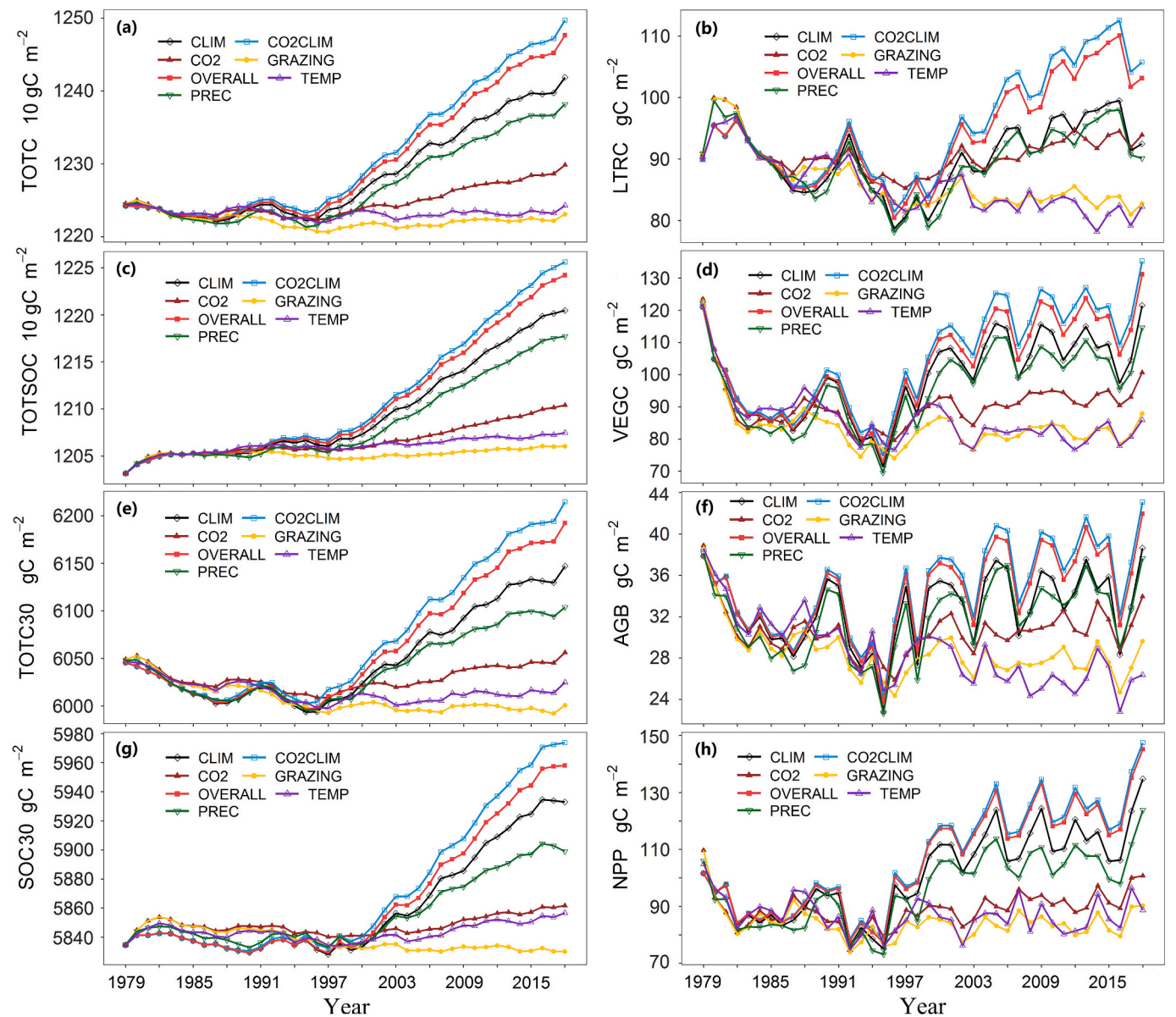


Fig. 4. Changes in total carbon (TOTC), litter carbon (LTRC), total soil organic carbon (TOTSOC), vegetation carbon (VEGC), total carbon above 30 cm soil depth (TOTC30), aboveground biomass (AGB), top layer (0–30 cm) soil organic carbon (SOC30), and net primary productivity (NPP) in the grasslands of the TP during 1979–2018 under different scenarios. (a) TOTC; (b) LTRC; (c) TOTSOC; (d) VEGC; (e) TOTC30; (f) AGB; (g) SOC30; (h) NPP. CLIM: S_{CLIM} scenario (black); CO2CLIM: $S_{CO2CLIM}$ scenario (blue); CO2: $S_{CO2fert}$ scenario (brown); GRAZING: $S_{GRAZING}$ scenario (yellow); OVERALL: $S_{OVERALL}$ scenario (red); TEMP: S_{TEMP} scenario (purple); PREC: S_{PREC} scenario (green).

Table 2
Average increase of carbon stocks ($g\ C\ m^{-2}$), AGB ($g\ C\ m^{-2}$), and NPP ($g\ C\ m^{-2}\ a^{-1}$) at the period 2000–2018, compared to the control scenario, from the Biome-BGCMuSo model output. The average was calculated across the whole spatial domain of the study area.

Scenarios	TOTC	TOTSOC	TOTC30	SOC30	LTRC	VEGC	AGB	NPP
$S_{CO2fert}$	32.4	19.3	23.4	11.1	6.1	7.0	2.6	6.4
S_{PREC}	89.2	63.6	60.0	34.4	6.1	19.5	5.3	21.6
S_{TEMP}	0.17	5.9	0.49	6.2	−2.7	−3.0	−2.0	0.9
S_{CLIM}	112.3	81.5	79.5	48.7	7.6	23.2	5.9	28.8
$S_{CO2CLIM}$	161.0	110.6	121.7	71.3	16.9	33.6	9.4	38.9
$S_{GRAZING}$	−11.7	−6.9	−12.4	−7.7	−1.8	−3.0	−0.7	−1.2

sequestration of alpine grasslands on the TP. In comparison to the $S_{CONTROL}$, the $S_{GRAZING}$ demonstrated a reduction in each carbon pool, NPP and AGB, with TOTC decreasing by $11.7\ g\ C\ m^{-2}$, NPP by $1.2\ g\ C\ m^{-2}\ a^{-1}$, and AGB by $0.7\ g\ C\ m^{-2}$, indicating that changes of the grazing intensity exert a detrimental influence on the carbon sinks of alpine

grasslands. This is why the values of the carbon pools, NPP, and AGB for $S_{OVERALL}$ were smaller than those for $S_{CO2CLIM}$. Nevertheless, the extent of this detrimental impact is considerably less pronounced than that of the $CO2fert_{effect}$ and $PREC_{effect}$.

Fig. 5 depicts the spatial variation patterns of TOTC, VEGC, AGB, and

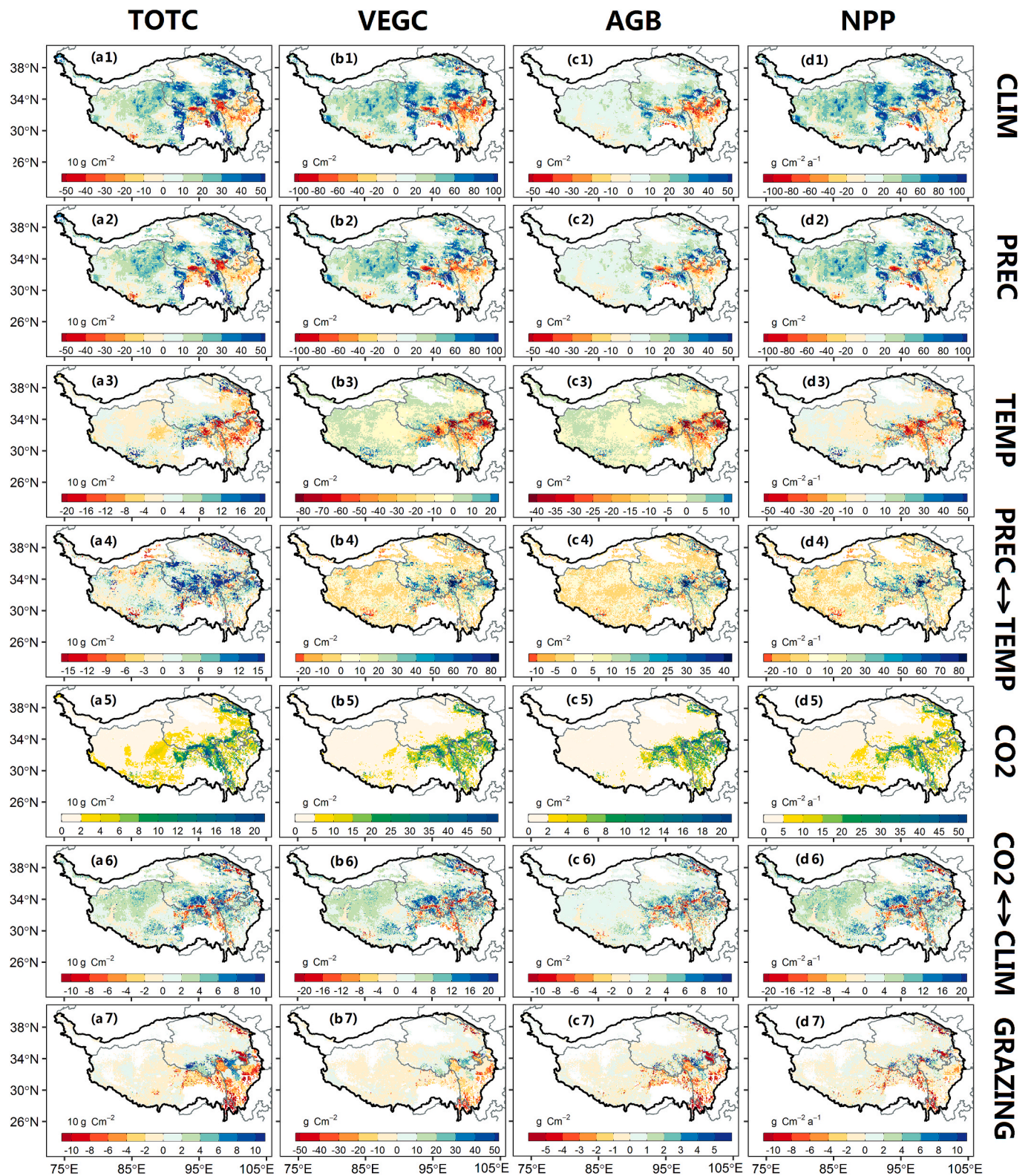


Fig. 5. Spatial patterns of TOTC (a1-a7), VEGC (b1-b7), AGB (c1-c7), and NPP (d1-d7) change (by comparing the mean values during the period 1979–1998 and 1999–2018), corresponding to the different experiments performed in this study. CLIM: climate change effect; PREC: precipitation change effect; TEMP: temperature change effect; PREC ↔ TEMP: the interactive effect between precipitation and temperature; CO₂: CO₂ change effect; CO₂ ↔ CLIM: the interactive effect between CO₂ change and climate change; GRAZING: the grazing intensity change effect.

NPP across a range of scenarios. The spatial distribution patterns of changes in TOTC, VEGC, AGB, and NPP due to climate change (Fig. 5a1, b1, c1, d1) and change of precipitation (Fig. 5a2, b2, c2, d2) exhibit notable similarities. For example, there were areas where the TOTC decreased by more than 300.0 g C m^{-2} , particularly along the border between the Qinghai and Sichuan Province (hereafter Sichuan) in the eastern TP (Fig. 5a1, a2). The regions exhibiting a reduction in TOTC were predominantly situated in areas experiencing a decline in precipitation, or in regions where the increase in precipitation fell below the 2.5 mm a^{-1} threshold (Fig. S8b). This suggests that precipitation plays a pivotal role in shaping the spatial distribution of carbon sinks. Conversely, warming led to significant reductions in TOTC, with some regions experiencing decreases of over 200.0 g C m^{-2} (Fig. 5a3). The most notable reductions were identified in the border regions of Tibet, Qinghai, and Sichuan, as well as in the northeastern Qinghai region. However, the warming resulted in a slight increase in AGB in northern Tibet and northern Qinghai, with gains of less than 5.0 g C m^{-2} (Fig. 5c3). It is noteworthy that the $\text{PREC} \leftrightarrow \text{TEMP}_{\text{effect}}$ generally resulted in an increase in TOTC across the TP, with values exceeding 150.0 g C m^{-2} in southern Qinghai (Fig. 5a4). With regard to the $\text{CO}_2\text{fert}_{\text{effect}}$, there was a notable increase in TOTC, VEGC, AGB, and NPP (Fig. 5a5, b5, c5, d5), particularly in regions with higher baseline values of VEGC and NPP. This indicates that the $\text{CO}_2\text{fert}_{\text{effect}}$ is more pronounced in regions with higher initial biomass, suggesting a strong relationship between $\text{CO}_2\text{fert}_{\text{effect}}$ and baseline vegetation productivity. In general, the $\text{CO}_2 \leftrightarrow \text{CLIM}_{\text{effect}}$ resulted in an increase in carbon pools, AGB and NPP, with some decreases observed along the Tibet-Sichuan border and in northeastern Qinghai (Fig. 5a6, b6, c6, d6). As a form of human activity disturbance, changes in grazing intensity, particularly in the northeastern Qinghai, Sichuan, and eastern Tibet, led to reductions in TOTC by over 100.0 g C m^{-2} in specific areas (Fig. 5a7). In contrast, specific areas in southern Qinghai showed significant increases in TOTC due to changes in grazing intensity.

3.3. Relevance and relative contributions of the factors to the changes in carbon stocks

Over the past four decades, the TP exhibited a trend of warming and increased precipitation, with temperatures rising by $0.4 \text{ }^\circ\text{C decade}^{-1}$ and precipitation by 3.31 mm a^{-1} , respectively (Figs. S7, S8). Precipitation

was the most influential factor explaining the increase of carbon stocks, NPP and AGB (Fig. 6). Precipitation positively contributed to the increases in TOTC, TOTSOC, TOTC30, SOC30, LTRC, VEGC, AGB, and NPP by 53.1 %, 56.6 %, 48.5 %, 45.7 %, 32.6 %, 46.4 %, 36.3 %, and 54.6 %, respectively. In contrast, the effect of rising temperature varied across different carbon pools. For AGB, NPP, and VEGC, the contributions of temperature were -22.3% , -4.6% , and -13.5% , respectively, suggesting that increased temperatures generally inhibit plant growth of alpine grasslands on the TP. However, TOTSOC and SOC30 increased with rising temperature (contribution of 2.6 % and 10.8 %, respectively), with a more pronounced impact for SOC30. On the other hand, TOTC decreased with warming (contribution of -2.7%), suggesting that the increases in TOTSOC were counteracted by reductions in VEGC and LTRC. Furthermore, the $\text{PREC} \leftrightarrow \text{TEMP}_{\text{effect}}$ was found to exceed the impact of temperature alone ($\text{TEMP}_{\text{effect}}$) in all cases except for AGB, with contributions ranging from 11.2 % to 19.2 % across various carbon-related variables. Additionally, this combined effect surpassed the $\text{CO}_2\text{fert}_{\text{effect}}$ on VEGC (16.3 % vs. 12.4 %), AGB (19.2 % vs. 13.1 %), and NPP (17.3 % vs. 12.4 %). This emphasizes the significance of the $\text{PREC} \leftrightarrow \text{TEMP}_{\text{effect}}$ on the alpine grasslands of the TP. While increased temperatures do not inherently stimulate plant growth and may even impede it, however, when increased temperatures coincide with increased precipitation, forming a ‘warm-wet’ climate trend, the combined effect of temperature and precipitation ($\text{CLIM}_{\text{effect}}$) outweighs the $\text{PREC}_{\text{effect}}$ in promoting plant growth. Moreover, the $\text{CO}_2 \leftrightarrow \text{CLIM}_{\text{effect}}$ had a positive impact on all carbon pools, NPP, and AGB. As a result, the combined effect of elevated CO_2 concentrations and a ‘warm-wet’ climate trend was greater than the sum of the $\text{CO}_2\text{fert}_{\text{effect}}$ and the $\text{CLIM}_{\text{effect}}$. With regard to grazing effect, changes in grazing intensity resulted in a reduction in all carbon pools, NPP, and AGB. It was found that changes in grazing intensity was the sole factor exerting a negative influence on SOC with negative contributions of -5.4% for TOTSOC and -7.7% for SOC30. The reduction in SOC promoted by changes in grazing intensity was lower in magnitude as compared to the increases of SOC promoted by the effects of $\text{PREC}_{\text{effect}}$, $\text{PREC} \leftrightarrow \text{TEMP}_{\text{effect}}$, $\text{CO}_2\text{fert}_{\text{effect}}$, and $\text{CO}_2 \leftrightarrow \text{CLIM}_{\text{effect}}$.

The spatial patterns of dominant controls on carbon dynamics across the TP were identified on a pixel-by-pixel basis (Fig. 7). The $\text{PREC}_{\text{effect}}$ was the dominant factor explaining the changes in TOTC, VEGC, AGB and NPP in the spatial domain, account for 67.9 %, 71.4 %, 71.4 %, and

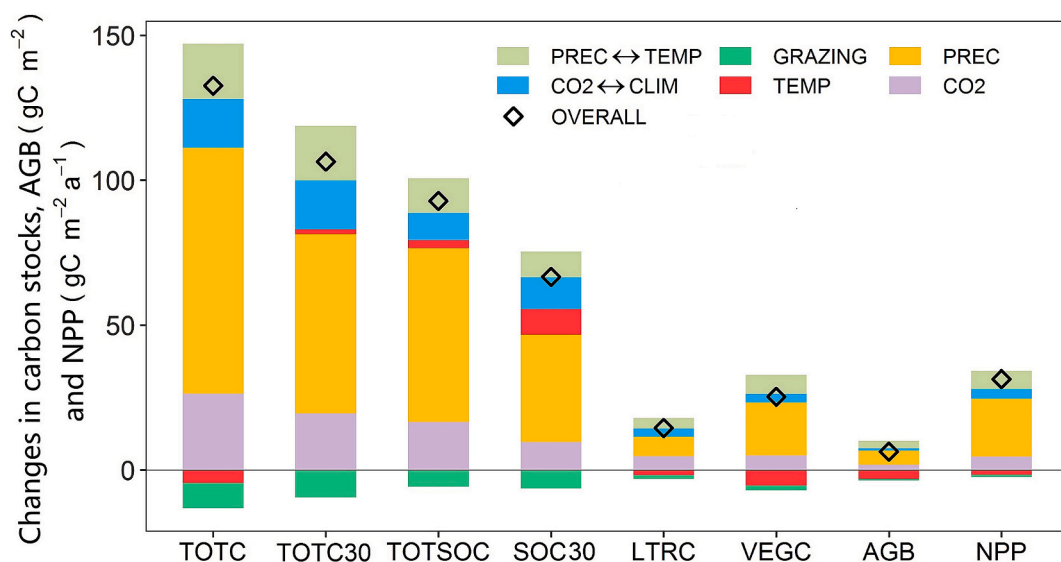


Fig. 6. The relative contributions of the individual and interactive environmental factors to carbon stocks, AGB and NPP. The changes in carbon stocks, AGB, and NPP were calculated by comparing the mean values for 1999–2018 with the average values for 1979–1998. OVERALL: combined effect; PREC: precipitation change effect (yellow); TEMP: temperature change effect (red); $\text{PREC} \leftrightarrow \text{TEMP}$: the interactive effect between precipitation and temperature (pale green); CO_2 : CO_2 change effect (purple); $\text{CO}_2 \leftrightarrow \text{CLIM}$: the interactive effect between CO_2 change and climate change (blue); GRAZING: the grazing intensity change effect (green).

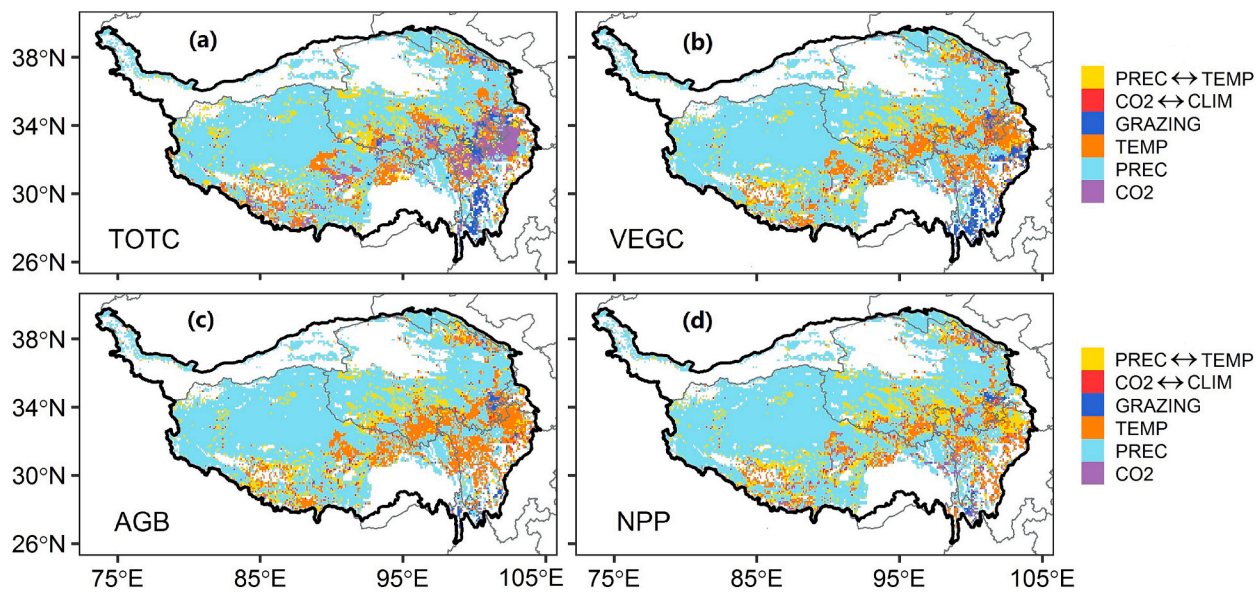


Fig. 7. Spatial pattern of the dominant factors on TOTC (a), VEGC (b), AGB (c), and NPP (d) over the grasslands of the Tibetan Plateau. PREC ↔ TEMP: the interactive effect between precipitation and temperature (yellow); CO₂ ↔ CLIM: the interactive effect between CO₂ change and climate change (red); GRAZING: the grazing intensity change effect (blue); TEMP: temperature change effect (brown); PREC: precipitation change effect (cyan); CO₂: CO₂ change effect (purple).

72.6 % of the study area, respectively. This area was located in northern Tibet and northern Qinghai. The TEMP_{effect} was the dominant factor for TOTC, VEGC, AGB, and NPP in 10.8 %, 11.7 %, 13.3 %, 15.4 %, and 10.8 % of the study area, respectively, located in southern Tibet, northeastern Qinghai, the border region between Qinghai and Sichuan, and Sichuan. The PREC ↔ TEMP_{effect} was the dominant factor for TOTC, VEGC, AGB, and NPP in 9.2 %, 9.4 %, 9.5 %, and 11.7 % of the study area, respectively. These areas were primarily distributed in southern Tibet and southern Qinghai. Changes in grazing intensity were the dominant factor for TOTC, VEGC, AGB, and NPP in 3.1 %, 3.4 %, 1.3 %, and 0.9 % of the study area, respectively, with these regions primarily located in Sichuan and Yunnan, where grazing intensity had decreased. The CO₂fert_{effect} was the dominant factor for TOTC, VEGC, AGB, and NPP in 7.4 %, 1.4 %, 0.9 %, and 2.6 % of the study area, respectively. Amongst all the factors, the CO₂ ↔ CLIM_{effect} had the least significant influence, accounting for less than 2 % of the alpine grasslands on the TP.

4. Discussion

4.1. Spatial distribution and influence of control factors on carbon dynamics

This study utilized the process-based model Biome-BGCMuSo to evaluate the spatial distribution of dominant drivers of carbon dynamics in alpine grasslands on the TP. Among the environmental factors considered, precipitation was identified as the most influential driver, affecting all carbon pools, AGB, and NPP (Fig. 6), and occupying the largest area as the dominant factor (Fig. 7). Specifically, increased precipitation (Fig. S8) was found to significantly enhance plant growth in northern Tibet and northern Qinghai, establishing PREC_{effect} as the dominant factor of carbon stocks and plant productivity in these regions (Fig. 7). This finding is consistent with evidence derived from remote sensing, field observations, and modeling. These studies demonstrated that, at the regional average level, precipitation plays a pivotal role in shaping carbon dynamics across the TP, exerting a greater influence than other environmental factors (He et al., 2023; Jiao et al., 2021; Li et al., 2020; Liu et al., 2021a; Shi et al., 2023; Shi et al., 2014). Increased precipitation increased soil moisture availability, which subsequently improves plant water conditions, thereby promoting growth (Fu et al.,

2018; Zhang et al., 2018). As a result of a high root/shoot ratio in alpine grasslands (e.g., in alpine meadows, the root/shoot ratio can reach up to 23.82), more biomass is allocated below ground, which directly enhances soil carbon input (Zhang et al., 2025). Increased water availability not only facilitated immediate plant growth but also contributed to an extended growing season. Specifically, increased precipitation prolonged the growing season of alpine grasslands on the TP, which further enhanced plant productivity (Meng et al., 2021; Peng et al., 2021a). As a consequence of the precipitation-driven increase in AGB and VEGC, LTRC also increases, leading to a greater carbon input to the soil, thereby increasing SOC, and ultimately resulting in an increase in TOTSOC and TOTC in response to increased precipitation (Chen et al., 2017). Consequently, precipitation was found to be the dominant driver of carbon dynamics in the alpine grasslands of the TP, highlighting its critical role in the carbon cycle of the region. The findings of our study suggested that precipitation dominates TOTC dynamics in 67.9 % of the grasslands on the TP, which is consistent with studies conducted in the largest temperate grassland belt in the world, the Central Asian grasslands (Zhu et al., 2023b). Precipitation dominated 59.0 % of the Central Asian grasslands primarily by reducing water stress and increasing plant productivity, while temperature dominated only 3.0 % of the Central Asian grasslands (Zhu et al., 2022). In contrast, Arctic tundra ecosystems, which are similar to the grassland ecosystems on the TP (e.g., cold climates, widespread permafrost, and substantial soil organic carbon stocks), are primarily influenced by temperature (Heffernan et al., 2024). This is due to distinct constraint mechanisms that differ from those governing the TP grasslands (Mishra et al., 2021).

The TEMP_{effect} on carbon dynamics in the alpine grasslands of the TP generally led to reductions in VEGC, AGB and NPP at the regional average scale, while exhibiting pronounced regional heterogeneity (Figs. 5, 6). Fu et al. (2015) demonstrated through field experiments that elevated temperatures have a detrimental impact on soil moisture of the grasslands, which in turn impede plant growth. In the central and eastern TP, where grassland productivity is relatively high, our model simulations indicated warming exacerbates the negative impacts on VEGC, AGB, and NPP by increasing water demand and intensifying soil moisture deficits. The limited warming reduces soil moisture in the upper layers through evapotranspiration, but it is not sufficient to disrupt the permafrost to replenish soil moisture. In the northern and western TP, where grassland productivity is lower than in the eastern TP

and vegetation is more drought-tolerant (Lin et al., 2023), our results showed that the negative effects of warming are less pronounced. In contrast to the findings of field experiments, which indicated that warming significantly stimulated plant growth in the alpine meadow but reduced growth in the alpine steppe, our model simulations revealed a different spatial pattern of $TEMP_{effect}$ (Chen et al., 2020; Ganjurjav et al., 2016). These differences can be attributed primarily to the fact that we compared vegetation and carbon stock simulations of the S_{TEMP} scenario between 1999–2018 and 1979–1998, while field experiments generally have shorter durations. Moreover, we used precipitation data reflecting 1979–1988 conditions under the S_{TEMP} scenario, which contrasts with field experiments where precipitation varied as well as temperature. Despite the reductions in plant growth, our findings indicated that warming increases TOTSOC and SOC, particularly in the surface soil layer (Fig. 6). The implication is that warming, which typically facilitates heterotrophic respiration by stimulating microbial decomposition, may impede heterotrophic respiration due to soil moisture deficiencies caused by warming and increased evapotranspiration (Chen et al., 2016; Chen et al., 2020). In summary, it is important to note that $TEMP_{effect}$ cannot be generalised across the entire alpine grasslands on the TP. Xie et al. (2024) revealed a clear spatiotemporal pattern of the temperature- and water-limitations: the eastern TP is characterized by temperature limitation (similar to the Arctic), whereas the western TP is characterized by water limitation (similar to the Central Asia). This explains why temperature is the key driver of TOTC in only 10.8 % of the TP, primarily in its eastern regions. In contrast to the circumpolar region, where temperature is the primary climatic factor influencing SOC stocks, Zhang et al. (2025) found precipitation determines the spatial variability of SOC of alpine grasslands on the TP. This may be attributed to harsher Arctic conditions, such as lower mean annual temperatures (-9.9°C in Arctic tundra compared to -3.5°C in grasslands on the TP), limited vegetation growth, and poorly developed soils, where increased precipitation does not significantly enhance VEGC and SOC (Mishra et al., 2021). Moreover, the longer SOC turnover times in the Arctic tundra compared to alpine grasslands on the TP (1609 vs. 547 years) may render Arctic SOC dynamics more sensitive to warming, as evidenced by a stronger correlation between turnover time with temperature in Arctic tundra than in the alpine grasslands of the TP ($R^2 = 0.44$ vs. $R^2 = 0.13$) (Wu et al., 2021). The spatial heterogeneity of $TEMP_{effect}$ emphasises the necessity of considering the regional context (including soil moisture availability, plant drought tolerance and regional climatic conditions) when evaluating the $TEMP_{effect}$ on the carbon dynamics of alpine grasslands.

Although the CO_2fert_{effect} was the dominant factor only in a relatively limited area (Fig. 7), its influence on carbon dynamics of alpine grasslands was considerable, particularly in its role in promoting plant growth and carbon sequestration. Our results demonstrated that CO_2fert_{effect} was the second most influential factor in regulating TOTC and LTRC, and the third most influential factor for NPP (Fig. 6). Our results further showed that the CO_2fert_{effect} is more pronounced in areas with higher biomass, thereby suggesting that regions with greater plant productivity are more responsive to elevated CO_2 levels (Fig. 5b5, c5, d5). This can be attributed to the fact that areas with higher biomass have greater photosynthetic capacity, which induces a larger requirement of CO_2 for growing, and increases CO_2 uptake by the growth. Nevertheless, the CO_2fert_{effect} is subject to modulation by other critical factors, including nitrogen availability and water supply. The results of CO_2 enrichment experiments conducted at the Naqu grassland station of northern TP indicated that nitrogen availability and precipitation exert a significant influence on the CO_2fert_{effect} , which is observed to diminish when water availability is high (Chen et al., 2021). Field experiments on the Naqu station further demonstrated that the combined addition of nitrogen and CO_2 enrichment results in a more pronounced increase in biomass than either factor alone (Zhu et al., 2020). This highlights the pivotal interaction between nutrient dynamics and CO_2fert_{effect} . Understanding how atmospheric CO_2 enrichment interacts with nitrogen

deposition and other environmental factors is essential for accurately predicting future carbon sequestration potential, particularly in view of the continued increase in global nitrogen deposition (Franz and Zaehle, 2021).

Previous studies have proposed that anthropogenic disturbance, predominantly grazing, exerts a dominant influence on the carbon dynamics of alpine grasslands on the TP (Liu et al., 2021b; Liu et al., 2019; Zhao et al., 2022). These studies primarily relied on Residuals-Trend model to assess vegetation dynamics. A meta-analysis of 136 paired observations from 55 publications quantified the impact of livestock grazing on SOC stocks and AGB in grasslands of the TP, revealing a significant decrease in SOC stock (11.9 %) and AGB (51.6 %) following grazing activities (Ma et al., 2022). However, this study specifically compared grazed versus ungrazed conditions, rather than examining the effects of varying grazing intensities. Our study demonstrated that changes in grazing intensity were not dominant factor influencing carbon dynamics in TP grasslands (Figs. 6, 7). This finding aligns with previous studies by Li et al. (2021b) and Zhang et al. (2017), which similarly indicated that grazing had a limited effect on carbon pools in comparison to climate factors, including precipitation and temperature. Lehnert et al. (2016) found that the dominant degradation pattern remained consistent across prefectures, irrespective of changes in livestock numbers. They concluded that climate variability, rather than overgrazing, was the primary driver of degradation between 2000 and 2013. In our study, although there was an increase/a reduction in grazing intensity over the TP, the change was minor compared to the historical baseline (Fig. S2), and thus had little impact on carbon dynamics at the regional scale (Meng et al., 2023). Nevertheless, there remains a significant debate in the scientific community about the relative contributions of grazing and natural environmental factors to carbon dynamics in grasslands on the TP (Li et al., 2018a). Further research is needed to clarify the potential long-term impacts of grazing on carbon sequestration potential. In particular, its interaction with other factors, such as precipitation and temperature, should be examined, especially in the context of grazing exclusion and ecological restoration in alpine grasslands.

In addition to quantifying the individual effects of different factors, we also assessed the $PREC \leftrightarrow TEMP_{effect}$ and $CO_2 \leftrightarrow CLIM_{effect}$ through factorial analysis. The findings demonstrate that for both VEGC and NPP, the $PREC \leftrightarrow TEMP_{effect}$ was the second most influential factor, indicating that warming can facilitate plant growth only when accompanied by increased precipitation (Fig. 6). The warming prolongs the growing season and facilitates photosynthesis in vegetation, thus increasing AGB and NPP (Peng et al., 2021a). However, warming also increases evapotranspiration, which could exacerbate drought conditions and reduce AGB and NPP if precipitation does not increase. By combining warming and increased precipitation, a longer growing season is maintained with vital water support. In the TP grasslands, where low temperatures typically limit decomposition, increased precipitation promotes plant growth and carbon input, often outweighing warming-induced acceleration of decomposition (Wei et al., 2021). Previous studies highlighted the significance of the $PREC \leftrightarrow TEMP_{effect}$. For instance, Li et al. (2020) found that the temperature had a positive influence on vegetation growth in humid regions but had a negative influence in arid regions, where water availability is limited. Similarly, Huang et al. (2016) found that in the arid northwestern TP, warming constrained vegetation growth, whereas in the relatively humid southeastern regions, warming had a positive effect on vegetation growth. A field experiment conducted by Zhao et al. (2019) at Nam Co Station revealed that a 2°C increase in temperature significantly reduced vegetation cover and AGB. However, when combined with a 15 % increase in precipitation, the detrimental effect of warming was offset, resulting in an enhanced vegetation growth. These results suggest that the $PREC \leftrightarrow TEMP_{effect}$ is crucial in determining plant productivity and carbon dynamics in the alpine grasslands on the TP. Similarly, in the Central Asian grasslands, the interactive effect was the most important

factor controlling TOTC and the second most important factor controlling NPP (Zhu et al., 2022). In the future, CMIP6 projections indicate an increase in precipitation and temperature over the TP (Huang et al., 2024). Given the positive effect of precipitation and the $\text{PREC} \leftrightarrow \text{TEMP}_{\text{effect}}$ on carbon uptake, the carbon sink capacity of the TP is expected to continue to increase in the future. Furthermore, the $\text{CO}_2 \leftrightarrow \text{CLIM}_{\text{effect}}$ also played a significant role in carbon dynamics (Fig. 6). While previous studies rarely focused on the $\text{CO}_2 \leftrightarrow \text{CLIM}_{\text{effect}}$ in detail, our study highlights its critical role in increasing carbon stocks, AGB, and NPP (Fig. 6). It is recommended that future research should prioritize a more in-depth exploration of these interactions in order to gain a deeper understanding of their implications for carbon dynamics under changing environmental conditions.

4.2. Uncertainties in the model and future prospects

In this study, AGB, SOC and NPP data were used exclusively for model evaluation and were not included in the model parameterization process. Given the temporal limitations of these datasets, particularly AGB, which is based on a single campaign, future research requires higher spatial resolution data and longer time series to improve model validation and reliability. The Biome-BGCMuSo model exhibited moderate performance in simulating AGB ($R^2 = 0.53$) and SOC ($R^2 = 0.56$). Two principal sources of discrepancies were identified in the validation of the field-observed AGB. Firstly, the model operated at a spatial resolution of 0.1° , whereas field measurements were conducted at each site within a $10 \text{ m} \times 10 \text{ m}$ area, leading to spatial scale mismatches that impact model performance. The TP is one of the regions with the highest surface roughness in the world (Amatulli et al., 2020). The analysis of elevation ranges within the CMFD grids ($0.1^\circ \times 0.1^\circ$), based on 90 m resolution SRTM DEM data, revealed considerable topographic heterogeneity in the grasslands of the TP. Specifically, 70.6 % of the grids showed elevation ranges greater than 500 m, and 34.9 % showed elevation ranges greater than 1000 m (Fig. S9). Secondly, the complex topography of the grasslands on the TP, with pronounced differences in NDVI between polar-facing slopes and equatorial-facing slopes (Yin et al., 2023), creates microclimatic conditions that are challenging to simulate in Biome-BGCMuSo model, further contributing to simulation discrepancies. With regards to the evaluation of SOC, it revealed uncertainties in the model arising from the complexity of subsurface processes and the multitude of biotic and abiotic interactions that regulate SOC input and turnover. The Multi-Scale Synthesis and Terrestrial Model Intercomparison Project (MsTMIP) revealed considerable inconsistency in the estimation of SOC across models, with estimates varying from less than 3 Pg C to over 40 Pg C on the TP (Ding et al., 2019). This variability reflects the challenges in accurately modelling SOC dynamics, which depend on the representation of decomposition rates and their sensitivity to temperature, soil moisture, and carbon–nitrogen interactions (Ito et al., 2020; Huntzinger et al., 2020; Moyano et al., 2013). Similarly, the Biome-BGCMuSo model may misrepresent the equilibrium between soil organic carbon accumulation and decomposition during the spin-up period, a limitation also observed in a case study using the LPJ-GUESS model in a boreal forest in southern Sweden (Islam et al., 2024). Such misrepresentation may result from uncertainties in the parameterization of SOC turnover rates and their sensitivity to environmental drivers, such as temperature and soil moisture (Huntzinger et al., 2020). These limitations highlight the need for improved model representations of SOC dynamics in Biome-BGCMuSo model, particularly in the alpine ecosystems of the TP, which are characterized by extreme climatic conditions, pronounced temperature variability and highly heterogeneous soils shaped by its unique topography.

In this study, grazing intensity data was obtained by interpolating GLW3 data using the county-level number of livestock recorded in statistical yearbooks, to generate regional-scale estimates of grazing intensity across the TP. Although this approach provides a comprehensive

method for estimating grazing intensity patterns over extensive areas, it still has certain limitations. Here, we highlight the potential of integrating remote sensing data to enhance grazing intensity assessments accuracy. For example, Chang et al. (2024) generated annual grazing probability and intensity maps based on Landsat 7/8 and Sentinel-2 images for the Hulun Buir grasslands in China. To improve the accuracy of future simulations of alpine grasslands on the TP, models and climate data should be downscaled to incorporate finer-scale details and topographic features into the analysis (Fiddes et al., 2022). The combination of advanced downscaling techniques with the integration of topographic corrections will facilitate a more detailed understanding of the carbon cycle dynamics of alpine grasslands on the TP (Tscholl et al., 2022), thereby supporting the development of more effective, localized management strategies for this vulnerable ecosystem.

5. Conclusion

The dominant drivers of alpine grassland carbon dynamics on the TP remains a subject of considerable debate. Using our 0.1° spatial resolution grazing intensity data for the TP, we parameterized grazing effects as a dynamic grazing pressure gradient within the Biome-BGCMuSo model. This study then separated and quantified the individual and interactive effects of climate change, atmospheric CO_2 enrichment, and grazing on carbon stocks, AGB, and NPP in the alpine grasslands of the TP through model scenarios and factor analysis. Our findings highlight the critical influence of precipitation on carbon dynamics across the region. The increased precipitation was identified as the primary driver of increasing carbon stocks, AGB, and NPP (positive contribution of 32.6–56.6 %). The sole effect of warming resulted in a decline in TOTC (negative contribution of -2.7 %), LTRC (-8.4 %), VEGC (-13.5 %), AGB (-22.3 %), and NPP (-4.6 %), particularly in the central and eastern TP. However, when warming was accompanied by increased precipitation, the interactive effects of precipitation and temperature increased carbon stocks, AGB and NPP (positive contribution of 10.9–19.2 %). This highlights the critical role of the synergistic interaction between precipitation and warming in driving positive changes in these ecosystems. CO_2 fertilization (positive contribution of 11.5–22.7 %), together with the interactive effects between CO_2 and climate change (positive contribution of 5.6–13.5 %), also showed positive effects on carbon dynamics, supporting further plant growth. In contrast, changes in grazing intensity were found to have a negative effect on carbon stocks, AGB and NPP; however, the impacts were limited. As projected by CMIP6, the future climate of the TP will become warmer and wetter. It is expected that AGB, NPP, and the carbon sequestration capacity of alpine grasslands will continue to increase due to the combined beneficial effects of increasing precipitation and its interaction with temperature. Under these conditions, a modest increase in grazing intensity could be feasible, potentially benefiting the livelihoods of herders while still maintaining the carbon sink function of alpine grasslands. Future studies should focus on disentangling the complex interactions between natural drivers and anthropogenic drivers, using high-resolution meteorological and grazing intensity data (e.g., 1 km spatial resolution). This will provide a deeper understanding of how alpine grassland ecosystems may respond to ongoing environmental changes and help refine predictions of carbon dynamics in alpine grasslands on the TP.

CRedit authorship contribution statement

Lei Zheng: Writing – original draft, Visualization, Software, Methodology, Formal analysis, Conceptualization. **Xiuliang Yuan:** Writing – review & editing. **Guoliang Wang:** Writing – review & editing, Funding acquisition. **Tiancai Zhou:** Writing – review & editing, Resources. **Yanyan Pei:** Writing – review & editing. **Shikai Song:** Writing – review & editing. **Yuzhen Li:** Writing – review & editing. **Shihua Zhu:** Writing – review & editing, Investigation. **Shangyu Shi:** Writing – review &

editing. **Jie Peng:** Writing – review & editing, Resources. **Yuyang Wang:** Writing – review & editing. **Jiaxing Zu:** Writing – review & editing. **Xiaoran Huang:** Writing – review & editing. **Qiang Yu:** Writing – review & editing, Funding acquisition.

Declaration of competing interest

The authors declare that they have no known competing financial interests or personal relationships that could have appeared to influence the work reported in this paper.

Acknowledgments

This study is funded by National Key Research and Development Program of China (2023YFB3907403), Startup Research Program of Northwest A&F University (2452023028), National Natural Science Foundation of China (NSFC) (42077456, 42205127), and the Hebei Natural Science Foundation (Grant No. D2021205013).

Appendix A. Supplementary data

Supplementary data to this article can be found online at <https://doi.org/10.1016/j.catena.2025.109376>.

Data availability

Carbon dynamics of grasslands on the Tibetan Plateau simulated by Biome-BGCMuSo (Original data) (Mendeley Data).

References

- Amatulli, G., McInerney, D., Sethi, T., Strobl, P., Domisch, S., 2020. Geomorpho90m, empirical evaluation and accuracy assessment of global high-resolution geomorphometric layers. *Sci. Data* 7 (1), 162. <https://doi.org/10.1038/s41597-020-0479-6>.
- Bohn, T.J., Livneh, B., Oyler, J.W., Running, S.W., Nijssen, B., Lettenmaier, D.P., 2013. Global evaluation of MTCLIM and related algorithms for forcing of ecological and hydrological models. *Agric. For. Meteorol.* 176, 38–49. <https://doi.org/10.1016/j.agrformet.2013.03.003>.
- Chang, C., Wang, J., Zhao, Y., Cai, T., Yang, J., Zhang, G., Zhang, Y., 2024. A 10-m annual grazing intensity dataset in 2015–2021 for the largest temperate meadow steppe in China. *Sci. Data* 11 (1), 181. <https://doi.org/10.1038/s41597-024-03017-5>.
- Chang, J., Ciais, P., Viovy, N., Vuichard, N., Herrero, M., Havlík, P., Soussana, J.F., 2016. Effect of climate change, CO₂ trends, nitrogen addition, and land-cover and management intensity changes on the carbon balance of European grasslands. *Glob. Chang. Biol.* 22 (1), 338–350. <https://doi.org/10.1111/gcb.13050>.
- Chen, B., Zhang, X., Tao, J., Wu, J., Wang, J., Shi, P., Yu, C., 2014. The impact of climate change and anthropogenic activities on alpine grassland over the Qinghai-Tibet Plateau. *Agric. For. Meteorol.* 189, 11–18. <https://doi.org/10.1016/j.agrformet.2014.01.002>.
- Chen, J.I., Luo, Y., Xia, J., Shi, Z., Jiang, L., Niu, S., Cao, J., 2016. Differential responses of ecosystem respiration components to experimental warming in a meadow grassland on the Tibetan Plateau. *Agric. For. Meteorol.* 220, 21–29. <https://doi.org/10.1016/j.agrformet.2016.01.010>.
- Chen, L., Jing, X., Flynn, D.F., Shi, Y., Kühn, P., Scholten, T., He, J.S., 2017. Changes of carbon stocks in alpine grassland soils from 2002 to 2011 on the Tibetan Plateau and their climatic causes. *Geoderma* 288, 166–174. <https://doi.org/10.1016/j.geoderma.2016.11.016>.
- Chen, Y., Feng, J., Yuan, X., Zhu, B., 2020. Effects of warming on carbon and nitrogen cycling in alpine grassland ecosystems on the Tibetan Plateau: a meta-analysis. *Geoderma* 370, 114363. <https://doi.org/10.1016/j.geoderma.2020.114363>.
- Chen, Y., Zhang, Y., Chen, N., Cong, N., Zhu, J., Zhao, G., Tang, Z., 2021. Nitrogen availability and precipitation variability regulated CO₂ fertilization effects on carbon fluxes in an alpine grassland. *Agric. For. Meteorol.* 307, 108524. <https://doi.org/10.1016/j.agrformet.2021.108524>.
- Ding, J., Wang, T., Piao, S., Smith, P., Zhang, G., Yan, Z., Zhao, L., 2019. The paleoclimatic footprint in the soil carbon stock of the Tibetan permafrost region. *Nat. Commun.* 10 (1), 4195. <https://doi.org/10.1038/s41467-019-12214-5>.
- Dong, S., Shang, Z., Gao, J., Boone, R.B., 2020. Enhancing sustainability of grassland ecosystems through ecological restoration and grazing management in an era of climate change on Qinghai-Tibetan Plateau. *Agric. Ecosyst. Environ.* 287, 106684. <https://doi.org/10.1016/j.agee.2019.106684>.
- Duan, A., Xiao, Z., 2015. Does the climate warming hiatus exist over the Tibetan Plateau? *Sci. Rep.* 5 (1), 13711. <https://doi.org/10.1038/srep13711>.
- Fang, X., Guo, X., Zhang, C., Shao, H., Zhu, S., Li, Z., He, B., 2019. Contributions of climate change to the terrestrial carbon stock of the arid region of China: a multi-dataset analysis. *Sci. Total Environ.* 668, 631–644. <https://doi.org/10.1016/j.scitotenv.2019.02.408>.
- Feng, H., Squires, V.R., 2020. Socio-environmental dynamics of alpine grasslands, steppes and meadows of the Qinghai-Tibetan Plateau, China: a commentary. *Appl. Sci.* 10 (18), 6488. <https://doi.org/10.3390/app10186488>.
- Fiddes, J., Aalstad, K., Lehning, M., 2022. TopoCLIM: rapid topography-based downscaling of regional climate model output in complex terrain v1.1. *Geosci. Model Dev.* 15 (4), 1753–1768. <https://doi.org/10.5194/gmd-15-1753-2022>.
- Franz, M., Zaehele, S., 2021. Competing effects of nitrogen deposition and ozone exposure on northern hemispheric terrestrial carbon uptake and storage, 1850–2099. *Biogeosciences* 18 (10), 3219–3241. <https://doi.org/10.5194/bg-18-3219-2021>.
- Friedlingstein, P., O'Sullivan, M., Jones, M.W., Andrew, R.M., Bakker, D.C., Hauck, J., et al., 2023. Global carbon budget 2023. *Earth Syst. Sci. Data* 15 (12), 5301–5369. <https://doi.org/10.5194/essd-15-5301-2023>.
- Fu, G., Shen, Z.X., Zhang, X.Z., 2018. Increased precipitation has stronger effects on plant production of an alpine meadow than does experimental warming in the Northern Tibetan Plateau. *Agric. For. Meteorol.* 249, 11–21. <https://doi.org/10.1016/j.agrformet.2017.11.017>.
- Fu, G., Sun, W., Yu, C.Q., Zhang, X.Z., Shen, Z.X., Li, Y.L., Zhou, N., 2015. Clipping alters the response of biomass production to experimental warming: a case study in an alpine meadow on the Tibetan Plateau, China. *J. Mt. Sci.* 12, 935–942. <https://doi.org/10.1007/s11629-014-3035-z>.
- Ganjurjav, H., Gao, Q., Gornish, E.S., Schwartz, M.W., Liang, Y., Cao, X., Lin, E., 2016. Differential response of alpine steppe and alpine meadow to climate warming in the central Qinghai-Tibetan Plateau. *Agric. For. Meteorol.* 223, 233–240. <https://doi.org/10.1016/j.agrformet.2016.03.017>.
- Ganjurjav, H., Gornish, E.S., Hu, G., Wan, Y., Li, Y., Danjiu, L., Gao, Q., 2018. Temperature leads to annual changes of plant community composition in alpine grasslands on the Qinghai-Tibetan Plateau. *Environ. Monit. Assess.* 190, 1–12. <https://doi.org/10.1007/s10661-018-6964-0>.
- Gilbert, M., Nicolas, G., Cinardi, G., Van Boeckel, T.P., Vanwambeke, S.O., Wint, G.R., Robinson, T.P., 2018. Global distribution data for cattle, buffaloes, horses, sheep, goats, pigs, chickens and ducks in 2010. *Sci. Data* 5 (1), 1–11. <https://doi.org/10.1038/sdata.2018.227>.
- Han, D., Hu, Z., Wang, X., Wang, T., Chen, A., Weng, Q., et al., 2022. Shift in controlling factors of carbon stocks across biomes on the Qinghai-Tibetan Plateau. *Environ. Res. Lett.* 17 (7), 074016. <https://doi.org/10.1088/1748-9326/ac78f5>.
- He, J., Yang, K., Tang, W., Lu, H., Qin, J., Chen, Y., Li, X., 2020. The first high-resolution meteorological forcing dataset for land process studies over China. *Sci. Data* 7 (1), 25. <https://doi.org/10.1038/s41597-020-0369-y>.
- He, L., Xie, Y., Wang, J., Zhang, J., Si, M., Guo, Z., et al., 2023. Precipitation regimes primarily drive the carbon uptake in the Tibetan Plateau. *Ecol. Ind.* 154, 110694. <https://doi.org/10.1016/j.ecolind.2023.110694>.
- Heffernan, E., Epstein, H., McQuinn, T.D., Rogers, B.M., Virkkala, A.M., Lutz, D., et al., 2024. Comparing assumptions and applications of dynamic vegetation models used in the Arctic-Boreal zone of Alaska and Canada. *Environ. Res. Lett.* 19 (9), 093003. <https://doi.org/10.1088/1748-9326/ad6619>.
- Hidy, D., Barcza, Z., Haszpra, L., Churkina, G., Pintér, K., Nagy, 2012. Development of the Biome-BGC model for simulation of managed herbaceous ecosystems. *Ecol. Model.* 226, 99–119. <https://doi.org/10.1016/j.ecolmodel.2011.11.008>.
- Hidy, D., Barcza, Z., Holló, R., Dobor, L., Ács, T., Zacháry, D., et al., 2022. Soil-related developments of the Biome-BGCMuSo v6.2 terrestrial ecosystem model. *Geosci. Model Dev.* 15 (5), 2157–2181. <https://doi.org/10.5194/gmd-15-2157-2022>.
- Hidy, D., Barcza, Z., Marjanović, H., Ostrogović Sever, M.Z., Dobor, L., Gelybó, G., et al., 2016. Terrestrial ecosystem process model Biome-BGCMuSo v4.0: summary of improvements and new modeling possibilities. *Geosci. Model Dev.* 9 (12), 4405–4437. <https://doi.org/10.5194/gmd-9-4405-2016>.
- Huang, B., Lu, F., Wang, X., Zheng, H., Wu, X., Zhang, L., et al., 2024. Ecological restoration is crucial in mitigating carbon loss caused by permafrost thawing on the Qinghai-Tibet Plateau. *Commun. Earth Environ.* 5 (1), 341. <https://doi.org/10.1038/s43247-024-01511-7>.
- Huang, K., Zhang, Y., Zhu, J., Liu, Y., Zu, J., Zhang, J., 2016. The influences of climate change and human activities on vegetation dynamics in the Qinghai-Tibet Plateau. *Remote Sens.* 8 (10), 876. <https://doi.org/10.3390/rs8100876>.
- Huang, W., Bruemmer, B., Huntsinger, L., 2017. Technical efficiency and the impact of grassland use right leasing on livestock grazing on the Qinghai-Tibetan Plateau. *Land Use Policy* 64, 342–352. <https://doi.org/10.1016/j.landusepol.2017.03.009>.
- Huntzinger, D.N., Schaefer, K., Schwalm, C., Fisher, J.B., Hayes, D., Stofferahn, E., Carey, J., Michalak, A.M., Wei, Y., Jain, A.K., Kolus, H., Mao, J., Poulter, B., Shi, X., Tang, J., Tian, H., 2020. Evaluation of simulated soil carbon dynamics in Arctic-Boreal ecosystems. *Environ. Res. Lett.* 15 (2), 025005. <https://doi.org/10.1088/1748-9326/ab6784>.
- Islam, M.R., Jonsson, A.M., Bergkvist, J., Lagergren, F., Lindeskog, M., Molder, M., Scholze, M., et al., 2024. Projected effects of climate change and forest management on carbon fluxes and biomass of a boreal forest. *Agric. For. Meteorol.* 349, 109959. <https://doi.org/10.1016/j.agrformet.2024.109959>.
- Ito, A., Hajima, T., Lawrence, D.M., Brovkin, V., Delire, C., Guenet, B., Jones, C.D., Malyshev, S., et al., 2020. Soil carbon sequestration simulated in CMIP6-LUMIP models: implications for climatic mitigation. *Environ. Res. Lett.* 15 (12), 124061. <https://doi.org/10.1088/1748-9326/abc912>.
- Jiao, K., Gao, J., Liu, Z., 2021. Precipitation drives the NDVI distribution on the Tibetan Plateau while high warming rates may intensify its ecological droughts. *Remote Sens.* 13 (7), 1305. <https://doi.org/10.3390/rs13071305>.
- Lehnert, L.W., Wesche, K., Trachte, K., Reudenbach, C., Bendix, J., 2016. Climate variability rather than overstocking causes recent large scale cover changes of Tibetan pastures. *Sci. Rep.* 6, 24367. <https://doi.org/10.1038/srep24367>.

- Li, L., Zhang, Y., Liu, L., Wu, J., Li, S., Zhang, H., et al., 2018a. Current challenges in distinguishing climatic and anthropogenic contributions to alpine grassland variation on the Tibetan Plateau. *Ecol. Evol.* 8 (11), 5949–5963. <https://doi.org/10.1002/ece3.4099>.
- Li, L., Zhang, Y., Liu, L., Wu, J., Wang, Z., Li, S., et al., 2018b. Spatiotemporal patterns of vegetation greenness change and associated climatic and anthropogenic drivers on the Tibetan Plateau during 2000–2015. *Remote Sens.* 10 (10), 1525. <https://doi.org/10.3390/rs10101525>.
- Li, M., Liu, S., Sun, Y., Liu, Y., 2021a. Agriculture and animal husbandry increased carbon footprint on the Qinghai-Tibet Plateau during past three decades. *J. Clean. Prod.* 278, 123963. <https://doi.org/10.1016/j.jclepro.2020.123963>.
- Li, M., Wu, J., Feng, Y., Niu, B., He, Y., Zhang, X., 2021b. Climate variability rather than livestock grazing dominates changes in alpine grassland productivity across Tibet. *Front. Ecol. Evol.* 9, 631024. <https://doi.org/10.3389/fevo.2021.631024>.
- Li, M., Zhang, X., Wu, J., Ding, Q., Niu, B., He, Y., 2021c. Declining human activity intensity on alpine grasslands of the Tibetan Plateau. *J. Environ. Manag.* 296, 113198. <https://doi.org/10.1016/j.jenvman.2021.113198>.
- Li, P., Hu, Z., Liu, Y., 2020. Shift in the trend of browning in Southwestern Tibetan Plateau in the past two decades. *Agric. For. Meteorol.* 287, 107950. <https://doi.org/10.1016/j.agrformet.2020.107950>.
- Lin, S., Wang, G., Hu, Z., Sun, X., Song, C., Huang, K., et al., 2023. Contrasting response of growing season water use efficiency to precipitation changes between alpine meadows and alpine steppes over the Tibetan Plateau. *Agric. Water Manag.* 289, 108571. <https://doi.org/10.1016/j.agwat.2023.108571>.
- Liu, Y., Liu, S., Sun, Y., Li, M., An, Y., Shi, F., 2021a. Spatial differentiation of the NPP and NDVI and its influencing factors vary with grassland type on the Qinghai-Tibet Plateau. *Environ. Monit. Assess.* 193, 1–21. <https://doi.org/10.1007/s10661-020-08824-y>.
- Liu, Y., Ren, H., Zheng, C., Zhou, R., Hu, T., Yang, P., et al., 2021b. Untangling the effects of management measures, climate and land use cover change on grassland dynamics in the Qinghai-Tibet Plateau, China. *Land Degrad. Dev.* 32 (17), 4974–4987. <https://doi.org/10.1002/ldr.4084>.
- Liu, Y., Wang, Q., Zhang, Z., Tong, L., Wang, Z., Li, J., 2019. Grassland dynamics in responses to climate variation and human activities in China from 2000 to 2013. *Sci. Total Environ.* 690, 27–39. <https://doi.org/10.1016/j.scitotenv.2019.06.503>.
- Ma, Z., Qin, W., Wang, Z., Han, C., Liu, X., Huang, X., 2022. A Meta-Analysis of Soil Organic Carbon Response to Livestock Grazing in Grassland of the Tibetan Plateau. *Sustainability* 14 (21), 14065. <https://doi.org/10.3390/su142114065>.
- Meng, F., Huang, L., Chen, A., Zhang, Y., Piao, S., 2021. Spring and autumn phenology across the Tibetan Plateau inferred from normalized difference vegetation index and solar-induced chlorophyll fluorescence. *Big Earth Data* 5 (2), 182–200. <https://doi.org/10.1080/20964471.2021.1920661>.
- Meng, N., Wang, L., Qi, W., Dai, X., Li, Z., Yang, Y., et al., 2023. A high-resolution gridded grazing dataset of grassland ecosystem on the Qinghai-Tibet Plateau in 1982–2015. *Sci. Data* 10 (1), 68. <https://doi.org/10.1038/s41597-023-01970-1>.
- Miehe, G., Miehe, S., Böhner, J., Kaiser, K., Hensen, I., Madsen, D., et al., 2014. How old is the human footprint in the world's largest alpine ecosystem? A review of multiproxy records from the Tibetan Plateau from the ecologists' viewpoint. *Quat. Sci. Rev.* 86, 190–209. <https://doi.org/10.1016/j.quascirev.2013.12.004>.
- Mishra, U., Hugelius, G., Shelef, E., Yang, Y., Strauss, J., Lupachev, A., et al., 2021. Spatial heterogeneity and environmental predictors of permafrost region soil organic carbon stocks. *Sci. Adv.* 7 (9), eaaz5236. <https://doi.org/10.1126/sciadv.aaz5236>.
- Moyano, F.E., Manzoni, S., Chenu, C., 2013. Responses of soil heterotrophic respiration to moisture availability: an exploration of processes and models. *Soil Biol. Biochem.* 59, 72–85. <https://doi.org/10.1016/j.soilbio.2013.01.002>.
- Pan, T., Zou, X., Liu, Y., Wu, S., He, G., 2017. Contributions of climatic and non-climatic drivers to grassland variations on the Tibetan Plateau. *Ecol. Eng.* 108, 307–317. <https://doi.org/10.1016/j.ecoleng.2017.07.039>.
- Peng, J., Wu, C., Wang, X., Lu, L., 2021a. Spring phenology outweighed climate change in determining autumn phenology on the Tibetan Plateau. *Int. J. Climatol.* 41 (6), 3725–3742. <https://doi.org/10.1002/joc.7045>.
- Peng, X., Frauenfeld, O.W., Jin, H., Du, R., Qiao, L., Zhao, Y., Zhang, T., 2021b. Assessment of temperature changes on the Tibetan Plateau during 1980–2018. *Earth Space Sci.* 8 (4), e2020EA001609. <https://doi.org/10.1029/2020EA001609>.
- Running, S.W., Zhao, M., 2015. Daily GPP and annual NPP (MOD17A2/A3) products NASA Earth observing system MODIS land algorithm. MOD17 User's Guide 2015, 1–28.
- Shangguan, W., Dai, Y., Liu, B., Ye, A., Yuan, H., 2012. A soil particle-size distribution dataset for regional land and climate modelling in China. *Geoderma* 171, 85–91. <https://doi.org/10.1016/j.geoderma.2011.01.013>.
- Shi, S., Wang, P., Zhan, X., Han, J., Guo, M., Wang, F., 2023. Warming and increasing precipitation induced greening on the northern Qinghai-Tibet Plateau. *Catena* 233, 107483. <https://doi.org/10.1016/j.catena.2023.107483>.
- Shi, Y., Wang, Y., Ma, Y., Ma, W., Liang, C., Flynn, D.F.B., et al., 2014. Field-based observations of regional-scale, temporal variation in net primary production in Tibetan alpine grasslands. *Biogeosciences* 11 (7), 2003–2016. <https://doi.org/10.5194/bg-11-2003-2014>.
- Sitch, S., O'sullivan, M., Robertson, E., Friedlingstein, P., Albergel, C., Anthoni, P., et al., 2024. Trends and drivers of terrestrial sources and sinks of carbon dioxide: an overview of the TRENDY project. *Glob. Biogeochem. Cycles* 38 (7), e2024GB008102. <https://doi.org/10.1029/2024GB008102>.
- Sun, J., Zhou, T., Liu, M., Chen, Y., Liu, G., Xu, M., et al., 2019. Water and heat availability are drivers of the aboveground plant carbon accumulation rate in alpine grasslands on the Tibetan Plateau. *Glob. Ecol. Biogeogr.* 29 (1), 50–64. <https://doi.org/10.1111/geb.13006>.
- Sun, Q., Li, B., Zhang, T., Yuan, Y., Gao, X., Ge, J., Li, F., Zhang, Z., 2017a. An improved Biome-BGC model for estimating net primary productivity of alpine meadow on the Qinghai-Tibet Plateau. *Ecol. Model.* 350, 55–68. <https://doi.org/10.1016/j.ecolmodel.2017.01.025>.
- Sun, Q., Li, B., Zhou, C., Li, F., Zhang, Z., Ding, L., et al., 2017b. A systematic review of research studies on the estimation of net primary productivity in the Three-River Headwater Region, China. *J. Geogr. Sci.* 27, 161–182. <https://doi.org/10.1007/s11442-017-1370-z>.
- The comprehensive scientific expedition team of the Qinghai Tibet Plateau, Chinese Academy of Sciences, 1992. *Grasslands in Tibet*. Science Press, Beijing (in Chinese).
- Trabucco, A., Zomer, R., 2019. Global aridity index and potential evapotranspiration (ETO) climate database v2. Figshare. Dataset. <https://doi.org/10.6084/m9.figshare.7504448.v3>.
- Tscholl, S., Tasser, E.I., Tappeiner, U., Vigl, L.E., 2022. Coupling solar radiation and cloud cover data for enhanced temperature predictions over topographically complex mountain terrain. *Int. J. Climatol.* 42 (9), 4684–4699. <https://doi.org/10.1002/joc.7497>.
- Wang, P., Wang, Z., Zhang, X., Feng, Q., Jiu, C., Chen, Q., 2010. GIS-based classification of seasonal pasture in Qinghai province. *Pratac. Sci.* 27 (02), 119–128 (in Chinese).
- Wang, S., Zhang, Y., Ju, W., Chen, J.M., Ciais, P., Cescatti, A., et al., 2020. Recent global decline of CO₂ fertilization effects on vegetation photosynthesis. *Science* 370 (6522), 1295–1300. <https://doi.org/10.1126/science.abb7772>.
- Wang, X., Pang, G., Yang, M., 2018. Precipitation over the Tibetan Plateau during recent decades: a review based on observations and simulations. *Int. J. Climatol.* 38 (3), 1116–1131. <https://doi.org/10.1002/joc.5246>.
- Wang, Y., Lv, W., Xue, K., Wang, S., Zhang, L., Hu, R., et al., 2022. Grassland changes and adaptive management on the Qinghai-Tibetan Plateau. *Nat. Rev. Earth Environ.* 3 (10), 668–683. <https://doi.org/10.1038/s43017-022-00330-8>.
- Wang, Y., Xiao, J., Ma, Y., Ding, J., Chen, X., Ding, Z., et al., 2023. Persistent and enhanced carbon sequestration capacity of alpine grasslands on Earth's Third Pole. *Sci. Adv.* 9 (20), eade6875. <https://doi.org/10.1126/sciadv.ade6875>.
- Wang, Z., Zhang, Y., Yang, Y., Zhou, W., Gang, C., Zhang, Y., et al., 2016. Quantitative assess the driving forces on the grassland degradation in the Qinghai-Tibet Plateau, China. *Ecol. Inform.* 33, 32–44. <https://doi.org/10.1016/j.ecoinf.2016.03.006>.
- Wei, D., Qi, Y., Ma, Y., Wang, X., Ma, W., Gao, T., et al., 2021. Plant uptake of CO₂ outpaces losses from permafrost and plant respiration on the Tibetan Plateau. *PNAS* 118 (33), e2015283118. <https://doi.org/10.1073/pnas.2015283118>.
- Wu, D., Liu, D., Wang, T., Ding, J., He, Y., Ciais, P., et al., 2021. Carbon turnover times shape topsoil carbon difference between Tibetan Plateau and Arctic tundra. *Sci. Bull.* 66 (16), 1698–1704. <https://doi.org/10.1016/j.scib.2021.04.019>.
- Xie, J., Yin, G., Ma, D., Chen, R., Zhao, W., Xie, Q., et al., 2024. Climatic limitations on grassland photosynthesis over the Tibetan Plateau shifted from temperature to water. *Sci. Total Environ.* 906, 167663. <https://doi.org/10.1016/j.scitotenv.2023.167663>.
- Xiong, Q., Xiao, Y., Liang, P., Li, L., Zhang, L., Li, T., et al., 2021. Trends in climate change and human interventions indicate grassland productivity on the Qinghai-Tibetan Plateau from 1980 to 2015. *Ecol. Ind.* 129, 108010. <https://doi.org/10.1016/j.ecolind.2021.108010>.
- Yang, Y., Fang, J., Fay, P.A., Bell, J.E., Ji, C., 2010. Rain use efficiency across a precipitation gradient on the Tibetan Plateau. *Geophys. Res. Lett.* 37 (15). <https://doi.org/10.1029/2010GL043920>.
- Yin, G., Yan, X., Ma, D., Xie, J., Chen, R., Pan, H., et al., 2023. Polar-facing slopes showed stronger greening trend than equatorial-facing slopes in Tibetan plateau grasslands. *Agric. For. Meteorol.* 341, 109698. <https://doi.org/10.1016/j.agrformet.2023.109698>.
- You, Q., Fraedrich, K.F., Ren, G., Pepin, N., Kang, S., 2013. Variability of temperature in the Tibetan Plateau based on homogenized surface stations and reanalysis data. *Int. J. Climatol.* 33 (6), 1337–1347. <https://doi.org/10.1002/joc.3512>.
- Yu, H., Ding, Q., Meng, B., Lv, Y., Liu, C., Zhang, X., et al., 2021. The relative contributions of climate and grazing on the dynamics of grassland NPP and PUE on the Qinghai-Tibet Plateau. *Remote Sens.* 13 (17), 3424. <https://doi.org/10.3390/rs13173424>.
- Zeng, N., Ren, X., He, H., Zhang, L., Zhao, D., Ge, R., et al., 2019. Estimating grassland aboveground biomass on the Tibetan Plateau using a random forest algorithm. *Ecol. Ind.* 102, 479–487. <https://doi.org/10.1016/j.ecolind.2019.02.023>.
- Zhang, F., Li, H., Zhu, J., Si, M., Fan, B., Zhou, H., et al., 2025. Precipitation determines the spatial variability of vegetation and topsoil organic carbon densities of Alpine Grasslands in the Qinghai-Tibetan Plateau, China. *Ecosystems* 28 (1), 1–12. <https://doi.org/10.1007/s10021-024-00957-2>.
- Zhang, T., Zhang, Y., Xu, M., Zhu, J., Chen, N., Jiang, Y., et al., 2018. Water availability is more important than temperature in driving the carbon fluxes of an alpine meadow on the Tibetan Plateau. *Agric. For. Meteorol.* 256, 22–31. <https://doi.org/10.1016/j.agrformet.2018.02.027>.
- Zhang, W., Zhang, F., Qi, J., Hou, F., 2017. Modeling impacts of climate change and grazing effects on plant biomass and soil organic carbon in the Qinghai-Tibetan grasslands. *Biogeosciences* 14 (23), 5455–5470. <https://doi.org/10.5194/bg-14-5455-2017>.
- Zhao, J., Luo, T., Wei, H., Deng, Z., Li, X., Li, R., Tang, Y., 2019. Increased precipitation offsets the negative effect of warming on plant biomass and ecosystem respiration in a Tibetan alpine steppe. *Agric. For. Meteorol.* 279, 107761. <https://doi.org/10.1016/j.agrformet.2019.107761>.
- Zhao, L., Liu, Z., Hu, Y., Zhou, W., Peng, Y., Ma, T., et al., 2022. Evaluation of reasonable stocking rate based on the relative contribution of climate change and grazing activities to the productivity of alpine grasslands in Qinghai province. *Remote Sens.* 14 (6), 1455. <https://doi.org/10.3390/rs14061455>.

- Zheng, J., Zhang, Y., Wang, X., Zhu, J., Zhao, G., Zheng, Z., et al., 2023. Estimation of net ecosystem productivity on the Tibetan Plateau Grassland from 1982 to 2018 based on random forest model. *Remote Sens.* 15 (9), 2375. <https://doi.org/10.3390/rs15092375>.
- Zheng, L., 2022. *Simulation of Impacts of Climate Change and Grazing on Net Primary Productivity, Carbon Stocks, and Aboveground Biomass of Grasslands over the Tibetan Plateau*. Institute of Geographic Sciences and Natural Resources Research. PhD Thesis.
- Zheng, L., Qi, Y., Wang, Y., Peng, J., Qin, Z., 2022. Calibration and validation of phenological models for Biome-BGCMuSo in the grasslands of Tibetan Plateau using remote sensing data. *Agric. For. Meteorol.* 322, 109001. <https://doi.org/10.1016/j.agrformet.2022.109001>.
- Zhou, W., Wang, T., Xiao, J., Wang, K., Yu, W., Du, Z., et al., 2024. Grassland productivity increase was dominated by climate in Qinghai-Tibet Plateau from 1982 to 2020. *J. Clean. Prod.* 434, 140144. <https://doi.org/10.1016/j.jclepro.2023.140144>.
- Zhu, J., Zhang, Y., Yang, X., Chen, N., Jiang, L., 2020. Synergistic effects of nitrogen and CO₂ enrichment on alpine grassland biomass and community structure. *New Phytol.* 228 (4), 1283–1294. <https://doi.org/10.1111/nph.16767>.
- Zhu, Q., Chen, H., Peng, C., Liu, J., Piao, S., He, J.S., et al., 2023a. An early warning signal for grassland degradation on the Qinghai-Tibetan Plateau. *Nat. Commun.* 14 (1), 6406. <https://doi.org/10.1038/s41467-023-42099-4>.
- Zhu, S., Chen, X., Zhang, C., Fang, X., Cao, L., 2022. Carbon variation of dry grasslands in Central Asia in response to climate controls and grazing appropriation. *Environ. Sci. Pollut. Res.* 29 (21), 32205–32219. <https://doi.org/10.1007/s11356-022-18542-2>.
- Zhu, S., Fang, X., Cao, L., Hang, X., Xie, X., Sun, L., Li, Y., 2023b. Multivariate drives and their interactive effects on the ratio of transpiration to evapotranspiration over Central Asia ecosystems. *Ecol. Model.* 478, 110294. <https://doi.org/10.1016/j.ecolmodel.2023.110294>.
- Zhu, Z., Piao, S., Myneni, R.B., Huang, M., Zeng, Z., Canadell, J.G., et al., 2016. Greening of the Earth and its drivers. *Nat. Clim. Chang.* 6 (8), 791–795. <https://doi.org/10.1038/nclimate3004>.